Stability, bifurcation and transition to chaos in a model of immunosensor based on lattice differential equations with delay

Vasyl Martsenyuk[✉][1], **Aleksandra Kłos-Witkowska**[1] and
Andriy Sverstiuk[2]

[1]University of Bielsko-Biala, Department of Computer Science and Automatics,
Faculty of Mechanical Engineering and Computer Science, Willowa Str 2, 43-309, Bielsko-Biala, Poland
[2]Ternopil State Medical University, Department of Medical Informatics,
Voli Square 1, 46001, Ternopil, Ukraine

Abstract. In the work we proposed the model of immunosensor, which is based on the system of lattice differential equations with delay. The conditions of local asymptotic stability for endemic state are gotten. For this purpose we have used method of Lyapunov functionals. It combines general approach to construction of Lyapunov functionals of the predator–prey models with lattice differential equations. Numerical examples have showed the influence on stability of model parameters. From our numerical simulations, we have found evidence that chaos can occur through variation in the time delay. Namely, as the time delay was increased, the stable endemic solution changed at a critical value of τ to a stable limit cycle. Further, when increasing the time delay, the behavior changed from convergence to simple limit cycle to convergence to complicated limit cycles with an increasing number of local maxima and minima per cycle until at sufficiently high time delay the behavior became chaotic.

Keywords: biosensor, immunosensor, lattice differential equations, differential equations with delay, asymptotic stability, Lyapunov functional, bifurcation, chaos.

2010 Mathematics Subject Classification: 92B05, 34K31, 34K20.

1   Introduction

With the growing pace of life and the need for more and more accurate detection methods, interest in biosensors is rising among science and industry as well. Biosensors are an alternative to commonly used measurement methods, which are characterized by: poor selectivity, high cost, poor stability, slow response and often can be performed only by highly trained personnel. They are a new generation of sensors, which use in their construction a biological material that provides a very high selectivity, also allow very quick and simple measurement

---

[✉]Corresponding author. Email: vmartsenyuk@ath.bielsko.pl

[40]. Biosensors are characterized by high versatility and therefore they are widely used in food industry [2] environmental protection [23], the defense industry, [9], but are most commonly used in medicine as a tool supporting making diagnoses [37]. In whole biosensor family there are two divisions. The first is related to the receptor layer and to the biological material used in its construction, which may be: enzyme, protein, porphyrin, antigen or antibody. The second is bound to the traducer layer, where the biological effect is converted on the measurable signal (electrochemical, impedance, amperometric, potentiometric optical biosensors or based on weight changed -piezoelectric biosensors).

1.1 Immunosensors structure and characteristics

Among large families of biosensors, immunosensors can be distinguished. In this type of sensor, receptor layer (sensitive, selective) contains an immobilized biological element (antibody, antigen or hapten), which are an immunological receptor for measurable molecules (analytes). In immunsor, the reaction based on the interaction between the antibody (Ab) and antigen (Ag) or small molecules (haptens) takes place. Antibodies are often called immunoglobulins, because they are proteins associated with the immune system. Immunoglobulins are used by the immune system to identify and neutralize foreign objects, they exhibit antigen binding properties. Both antigens and antibodies can be used in the receptor layer in biosensors. However, because of the loss of antibodies attractive properties during the immobilization process the antigens are used in receptor layer construction, whereas antibodies generally play a function of analytes (molecules subject to detection) [39]. During the detection process, combining antibodies with antigen leads to complex formation The binding between the antigen and the antibody is very strong, the binding constant is $Ka = 10^{-12} - 10^{-14}$ [24].

1.2 Qualitative investigations of predator–prey models

Since a predator–prey model is the main counterpart of the proposed model in the work, that will be used for description of immunosensor pixel, we present here the main results dealing with its stability investigation.

The most of results dealing with stability investigation of predator–prey models are stated with help of the basic reproduction numbers. There are different approaches to calculate the basic reproduction number. Below we pay Your attention to ones which are dealt with our problem. One of the most common definition of the basic reproduction number was introduced in [13]. The basic reproduction number is mathematically defined as the dominant eigenvalue of a positive linear operator (so called next-generation operator). It was shown that in certain special cases one can easily compute or estimate this eigenvalue.

In [35] they used approach based on next-generation operator [13] for computing the basic reproduction numbers for SI epidemic models with distributed and discrete delays. The originality of the works, which study epidemic systems with distributed delay [6,32], is to have a basic reproduction number $\mathcal{R}_0$ which depends on the distribution of the latent period. So, in [32] the model of infectious disease with distributed delays is considered which uses gamma function as distribution functions. For the different values of the basic reproduction number and the second basic reproduction number, there are investigated the stability of the infection-free equilibrium, the single-infection equilibrium and the double infection equilibrium. It was concluded that increasing delays will decrease the values of the basic reproduction number and the second basic reproduction number.

One of the most general models with discrete time delays is considered in [38]. The basic reproduction numbers are introduced for all five counterparts of the model. In [18] the model makes use of the more realistic standard incidence function and explicitly incorporates a discrete time delay in virus production. As a result, the infection reproduction number is explicitly dependent on the time delay. But we note that this is only a consequence of the explicit incorporation of the time delay into the parameters of the model.

In [21] the basic reproduction numbers are introduced for SIR epidemic model with distributed time delay on complex population networks. Under this framework, each node of the network represents an individual in its corresponding state (susceptible, infected, or removed), possible contacts between two individuals are linked by an edge, and these two nodes are called neighbors of each other. Each edge is a connection along which the infection can spread, thus a node can acquire infection only from one of its neighbors, in other words, the contact rate is proportional to the number of neighbors, i.e. the degree of a node. Despite the complex population networks are close to lattices, this approach is not appropriate for our work because it describes only amount of the nodes of the certain degree. Further in the work we will use an approach which is offered in [54] for delayed system. In order to calculate $\mathcal{R}_0$ it does not use the values of parameters directly, but the steady states themselves. We will try to extend it to lattice equations.

We pay especial attention primarily on approaches of Lyapunov functional construction [1, 16, 46–48]. One of the current survey on Lyapunov functional for predator–prey models with delays you can find in [49] (see pp. 43–44). When considering predator–prey models without delay, then using the direct Lyapunov method with Volterra type Lyapunov functions, we can establish conditions for the global stability of an endemic steady state [25, 26, 28]. The most general results were received by A. Korobeinikov for functional responses of a general nonlinear form without delays in [27].

There were a few attempts to develop Lyapunov functionals for predator–prey models with delays using Volterra type Lyapunov functions as prototypes. Here we present two the most significant of them. The papers [35, 36] presented an SIR model of disease transmission with delay and nonlinear incidence. The analysis there resolves the global stability of the endemic equilibrium for the case where the reproduction number $\mathcal{R}_0$ is greater than one. In such a case the global dynamics are fully determined for $\mathcal{R}_0 > 1$ by using a Lyapunov functional. It was shown that the endemic equilibrium is globally asymptotically stable whenever it exists.

In [49] the global asymptotic stability of delay Lotka–Volterra-type cooperative systems with discrete delays are carried out via the construction of a suitable Lyapunov functional, obtained from the appropriate combination of the elegant Lyapunov function

$$\tilde{L}(t) = \ln \frac{n}{n^\star} + \frac{n^\star}{n} - 1$$

and the Volterra-type Lyapunov functional

$$W^+(t) = \int_0^\tau \left[\frac{n(t-w)}{n^\star} - 1 - \ln \frac{n(t-w)}{n^\star} \right] dw$$

In the work [19] sufficient conditions for both local and global stability of the positive equilibrium in a predator–prey system with time delays

$$\begin{aligned}
\frac{dN_1(t)}{dt} &= N_1(t)\left[a_1 - b_1 N_1(t-\tau) - c_1 N_2(t-\sigma) \right], \\
\frac{dN_2(t)}{dt} &= N_2(t)\left[-a_2 + c_2 N_1(t-\sigma) - b_2 N_2(t) \right]
\end{aligned}$$

(1.1)

with nonnegative initial conditions (positive at $t = 0$) are obtained by constructing suitable Lyapunov functionals.

In [51] this technique of construction of Lyapunov functionals was applied for the predator–prey system with Michaelis–Menten type functional response

$$\dot{x}_1 = x_1(t)\left(a_1 - a_{11}x_1\left(t - \tau_{11} - \frac{a_{12}x_2(t)}{m_1 + x_1(t)}\right)\right),$$

$$\dot{x}_2 = x_2(t)\left(-a_2 + \frac{a_{21}x_1(t - \tau_{21})}{m_1 + x_1(t - \tau_{21})} - a_{22}x_2(t - \tau_{22}) - \frac{a_{23}x_3(t)}{m_2 + x_2(t)}\right),$$

$$\dot{x}_3 = x_3(t)\left(-a_3 + \frac{a_{32}x_2(t - \tau_{32})}{m_2 + x_2(t - \tau_{32})} - a_{33}x_3(t - \tau_{33})\right).$$

In [52] it was used for Holling-type 3 functional response

$$\dot{x}_1(t) = x_1(t)\left(a_1 - a_{11}x_1(t - \tau_1) - a_{12}\frac{x_1(t)x_2(t)}{m + x_1^2(t)}\right),$$

$$\dot{x}_2(t) = x_2(t)\left(-a_2 + a_{21}\frac{x_1^2(t - \tau_2)}{m + x_1^2(t - \tau_2)} - a_{22}x_2(t - \tau_3)\right).$$

The last approach will be partially used for lattice model offered further in the given paper.

Bifurcation and chaos are important phenomena affecting many predator–prey systems. They are also related to the stability and multiplicity phenomena associated with these systems. The phenomena are not only of theoretical or mathematical interest but are also important for experimental research and design (for example, biosensor design). In the last few years, researchers have been showing keen interest to investigate the bifurcations and the transition to chaos arising from the delayed predator–prey systems.

In [4,53] it was proved that the ratio-dependent predator–prey systems with constant delay undergoes a Hopf bifurcation at the positive equilibrium. Using the normal form theory and the center manifold reduction, explicit formulae were derived to determine the direction of bifurcations and the stability and other properties of bifurcating periodic solutions. A chaotic behavior occurs in the ratio-dependent predator–prey model with stage-structured predators and constant delay. Numerical simulations of the work [8] showed that the behavior of such system can become extremely complicated as the time delay is increased, with the long-time behavior changing from a stable coexistence equilibrium, to a limit cycle with one local maximum and minimum per cycle (Hopf bifurcation), to limit cycles with an increasing number of local maxima and minima per cycle, and finally to chaotic-type solutions. In the works [10, 29] predator–prey models with distributed delay were investigated. For such systems numerical solutions revealed the existence of stable periodic attractors, attractors at infinity, as well as bounded chaotic dynamics in various cases.

1.3   Lattice differential equations

Lattice differential equations arise in many applied subjects, such as chemical reaction, image processing, material science, and biology [42]. In the models of lattice differential equations, the spatial structure has a discrete character, and lattice dynamics have recently been extensively used to model biological problems [11,20,42,44,50,55] since the environment in which the species population lives may be discrete but not continuous.

2   Lattice model of antibody–antigen interaction for two-dimensional biopixels array

Let $V_{i,j}(t)$ be concentration of antigens, $F_{i,j}(t)$ be concentration of antibodies in biopixel (i,j), $i,j = \overline{1,N}$.

The model is based on the following biological assumptions for arbitrary biopixel (i,j).

1. We have some constant birthrate $\beta > 0$ for antigen population.

2. Antigens are detected, binded and finally neutralized by antibodies with some probability rate $\gamma > 0$.

3. We have some constant death rate of antibodies $\mu_f > 0$.

4. We assume that when the antibody colonies are absent, the antigen colonies are governed by the well known delay logistic equation:

$$\frac{dV_{i,j}(t)}{dt} = (\beta - \delta_v V_{i,j}(t - \tau))V_{i,j}(t), \tag{2.1}$$

   where β and δ_v are positive numbers and $\tau \geq 0$ denotes delay in the negative feedback of the antigen colonies.

5. The antibody decreases the average growth rate of antigen linearly with a certain time delay τ; this assumption corresponds to the fact that antibodies cannot detect and bind antigen instantly; antibodies have to spend τ units of time before they are capable of decreasing the average growth rate of the antigen colonies; these aspects are incorporated in the antigen dynamics by the inclusion of the term $-\gamma F_{i,j}(t - \tau)$ where γ is a positive constant which can vary depending on the specific colonies of antibodies and antigens.

6. In the absence of antigen colonies, the average growth rate of the antibody colonies decreases exponentially due to the presence of $-\mu_f$ in the antibody dynamics and so as to incorporate the negative effects of antibody crowding we have included the term $-\delta_f F_{i,j}(t)$ in the antibody dynamics.

7. The positive feedback $\eta \gamma V_{i,j}(t - \tau)$ in the average growth rate of the antibody has a delay since mature adult antibodies can only contribute to the production of antibody biomass; one can consider the delay τ in $\eta \gamma V_{i,j}(t - \tau)$ as a delay in antibody maturation.

8. While the last delay need not be the same as the delay in the hunting term and in the term governing antigen colonies, we have retained this for simplicity. We remark that the delays in the antibody term, antibody replacement term and antigen negative feedback term can be made different and a similar analysis can be followed.

9. We have some diffusion of antigens from four neighboring pixels $(i - 1, j)$, $(i + 1, j)$, $(i, j - 1)$, $(i, j + 1)$ (see Fig. 2.1) with diffusion $D > 0$. Here we consider only diffusion of antigens, because the model describes so-called "competitive" configuration of immunosensor [12]. When considering competitive configuration of immunosensor, the factors immobilized on the biosensor matrix are antigens, while the antibodies play the role of analytes or particles to be detected.
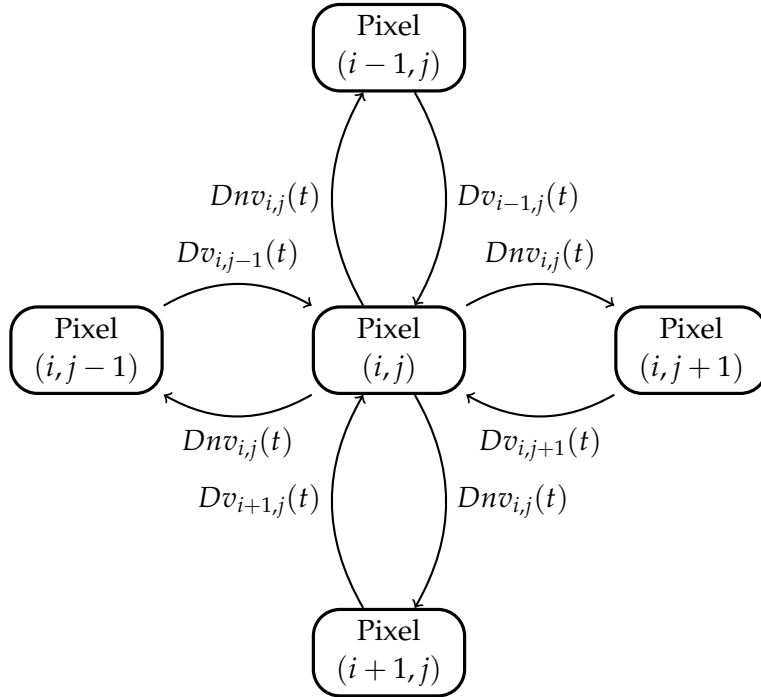
Figure 2.1: Linear lattice interconnected four neighboring pixels model, $n > 0$ is the disbalance constant

10. We consider surface lateral diffusion (movement of molecules on the surface on solid phase toward an immobilized molecules) [43]. Moreover, there are works [5,7] which assume and consider surface diffusion as an entirely independent stage.

11. We extend definition of usual diffusion operator in case of surface diffusion in the following way. Let $n \in (0,1]$ be a factor of diffusion disbalance. It means that only nth portion of antigens of the pixel (i,j) may be included into diffusion process to any neighboring pixel as a result of surface diffusion.

For the reasonings given we consider a very simple delayed antibody–antigen competition model for biopixels two-dimensional array which is based on well-known Marchuk model [15,33,34,41] and using spatial operator $\hat{S}$ offered in [45] (Supplementary information, p. 10).

$$\frac{dV_{i,j}(t)}{dt} = (\beta - \gamma F_{i,j}(t-\tau) - \delta_v V_{i,j}(t-\tau))V_{i,j}(t) + \hat{S}\{V_{i,j}\},$$
$$\frac{dF_{i,j}(t)}{dt} = \left(-\mu_f + \eta\gamma V_{i,j}(t-\tau) - \delta_f F_{ij}(t)\right)F_{i,j}(t) \tag{2.2}$$

with given initial functions

$$V_{i,j}(t) = V_{i,j}^0(t) \geq 0, \quad F_{i,j}(t) = F_{i,j}^0(t) \geq 0, \quad t \in [-\tau, 0),$$
$$V_{i,j}(0), F_{i,j}(0) > 0. \tag{2.3}$$

For a square $N \times N$ array of traps, we use the following discrete diffusion form of the

spatial operator [45]

$$
\hat{S}\{V_{i,j}\} =
\begin{cases}
D\left[V_{1,2} + V_{2,1} - 2nV_{1,1}\right], & i,j = 1 \\[4pt]
D\left[V_{2,j} + V_{1,j-1} + V_{1,j+1} - 3nV_{i,j}\right], & i = 1, j \in \overline{2, N-1} \\[4pt]
D\left[V_{1,N-1} + V_{2,N} - 2nV_{1,N}\right], & i = 1, j = N \\[4pt]
D\left[V_{i-1,N} + V_{i+1,N} + V_{i,N-1} - 3nV_{i,N}\right], & i \in \overline{2, N-1}, j = N \\[4pt]
D\left[V_{N-1,N} + V_{N,N-1} - 2nV_{N,N}\right] & i = N, j = N \\[4pt]
D\left[V_{N-1,j} + V_{N,j-1} + V_{N,j+1} - 3nV_{N,j}\right], & i = N, j \in \overline{2, N-1} \\[4pt]
D\left[V_{N-1,1} + V_{N,2} - 2nV_{N,1}\right], & i = N, j = 1 \\[4pt]
D\left[V_{i-1,1} + V_{i+1,1} + V_{i,2} - 3nV_{i,1}\right], & i \in \overline{2, N-1}, j = 1 \\[4pt]
D\left[V_{i-1,j} + V_{i+1,j} + V_{i,j-1} + V_{i,j+1} - 4nV_{i,j}\right], & i,j \in \overline{2, N-1}.
\end{cases}
\tag{2.4}
$$

Each colony is affected by the antigen produced in four neighboring colonies, two in each dimension of the array, separated by the equal distance Δ. We use the boundary condition $V_{i,j} = 0$ for the edges of the array $i,j = 0, N+1$. Further we will use the following notation of the constant

$$
k(i,j) =
\begin{cases}
2, & i,j = 1; \quad i = 1, j = N; \quad i = N, j = N; \quad i = N, j = 1, \\[4pt]
3, & i = 1, j \in \overline{2, N-1}; \quad i \in \overline{2, N-1}, j = N; \quad i = N, j \in \overline{2, N-1}; \\
& i \in \overline{2, N-1}, j = 1 \\[4pt]
4, & i,j \in \overline{2, N-1}
\end{cases}
\tag{2.5}
$$

which will be used in manipulations with the spatial operator (2.4).

Results of modeling (2.2) are presented in Section 4. It can be seen that qualitative behavior of the system is determined mostly by the time of immune response τ (or time delay), diffusion D and constant n.

3   Stability problem in immunosensors

In the context of biosensors two types of stability can be distinguished: self stability and operational stability. Self stability is defined as the enhancement or improvement of activity retention of an enzyme, protein, diagnostic or device when stored under specific condition. Operational stability is the retention of activity when in use [17]. The stability of the sensible element located in the biosensor receptor layer and the stability associated with the activity of the biosensor matrix components during use, determine the usefulness of the device

Qualitative results which are obtained hereinafter can be applied for both types of stability. Namely, simulation of different types of stability problems can be implemented through different initial conditions for pixels (especially for boundary pixels).

3.1 Steady states

The steady states of the model (2.2) are the intersection of the null-clines $dV_{i,j}(t)/dt = 0$ and $dF_{i,j}(t)/dt = 0$, $i, j = \overline{1, N}$.

Antigen-free steady state. If $V_{i,j}(t) \equiv 0$, the free antigen equilibrium is at $\mathcal{E}^0_{i,j} \equiv (0,0)$, $i, j = \overline{1, N}$ or $\mathcal{E}^0_{i,j} \equiv (0, -\frac{\mu_f}{\delta_f})$, $i, j = \overline{1, N}$. The last solution does not have biological sense and can not be reached for nonnegative initial conditions (2.3).

When considering endemic steady state $\mathcal{E}^*_{i,j} \equiv (V^*_{i,j}, F^*_{i,j})$, $i, j = \overline{1, N}$ for (2.2) we get the algebraic system:

$$\left(\beta - \gamma F^*_{i,j} - \delta_v V^*_{i,j}\right) V^*_{i,j} + \hat{S}\left\{V^*_{i,j}\right\} = 0,$$
$$\left(-\mu_f + \eta\gamma V^*_{i,j} - \delta_f F^*_{i,j}\right) F^*_{i,j} = 0, \quad i, j = \overline{1, N}. \tag{3.1}$$

The solutions $(V^*_{i,j}, F^*_{i,j})$ of (3.1) can be found as a result of solving lattice equation with respect to $V^*_{i,j}$, and using relation $F^*_{i,j} = \frac{-\mu_f + \eta\gamma V^*_{i,j}}{\delta_f}$

Then we have to differ two cases.

Identical endemic state for all pixels. Let us assume there is the solution of (3.1) $V^*_{i,j} \equiv V^*$, $F^*_{i,j} \equiv F^*$, $i, j = \overline{1, N}$, i.e., $\hat{S}\{V^*_{i,j}\} \equiv 0$. Then $\mathcal{E}^*_{i,j} = (V^*, F^*)$, $i, j = \overline{1, N}$ can be calculated as

$$V^* = \frac{-\beta\delta_f - \gamma\mu_f}{\delta_v\delta_f - \eta\gamma^2}, \quad F^* = \frac{\delta_v\mu_f - \eta\gamma\beta}{\delta_v\delta_f - \eta\gamma^2}. \tag{3.2}$$

provided that $\delta_v\delta_f - \eta\gamma^2 < 0$.

Nonidentical endemic state for pixels. In general case we have endemic steady state which is different from (3.2). It is shown numerically in Section 4 that it appears as a result of diffusion between pixels D.

At absence of diffusion, i.e. $D = 0$, we have only identical endemic state for pixels of external layer. At presence of diffusion $D > 0$ nonidentical endemic states tends to identical one (3.2) at internal pixels, which can be observed at numerical simulation. This phenomenon is clearly appeared at bigger amount of pixels.

3.2 Basic reproduction numbers

Here we define the basic reproduction number for antigen colony which is localized in pixel (i, j).

When considering epidemic models, the basic reproduction number, $\mathcal{R}_0$, is defined as the expected number of secondary cases produced by a single (typical) infection in a completely susceptible population. It is important to note that $\mathcal{R}_0$ is a dimensionless number [22]. When applying this definition to the pixel (i, j), which is described by the equation (2.2), we get

$$\mathcal{R}_{0,i,j} = \mathcal{T}_{i,j}\bar{c}_{i,j}, d_{i,j}$$

where $\mathcal{T}_{i,j}$ is the transmissibility (i.e., probability of binding given constant between an antigen and antibody), $\bar{c}_{i,j}$ is the average rate of contact between antigens and antibodies, and $d_{i,j}$ is the duration of binding of antigen by antibody till deactivation.

Unfortunately, the lattice system (2.2) does not include all parameters, which allow to calculate the basic reproduction numbers in a clear form. Firstly, let us consider pixel $(i^\star, j^\star)$ without diffusion, i.e., $\hat{S}\{V_{i^\star, j^\star}\} \equiv 0$. In this case the non-negative equilibria of (2.2) are

$$\mathcal{E}^0_{i^\star, j^\star} = (V^0, 0) := \left(\frac{\beta}{\delta_v}, 0\right), \qquad \mathcal{E}^\star_{i^\star, j^\star} = (V^\star, F^\star).$$

Due to the approach which was offered in [54] (in pages 4 for ordinary differential equations, 5 for delay model), we introduce the basic reproduction number for pixel $(i^\star, j^\star)$ without diffusion, which is given by expression

$$\mathcal{R}_{0, i^\star, j^\star} := \frac{V^0}{V^\star} = \frac{\beta}{\delta_v V^\star} = \frac{\beta(\eta\gamma^2 - \delta_v\delta_f)}{\delta_v(\beta\delta_f + \gamma\mu_f)}.$$

Its biological meaning is given as being the average number of offsprings produced by a mature antibody in its lifetime when introduced in a antigen-only environment with antigen at carrying capacity.

According to the common theory it can be shown that antibody-free equilibrium $\mathcal{E}^0_{i^\star, j^\star}$ is locally asymptotically stable if $\mathcal{R}_{0, i^\star, j^\star} < 1$ and it is unstable if $\mathcal{R}_{0, i^\star, j^\star} > 1$. It can be done with help of analysis of the roots of characteristic equation (similarly to [54, p. 5]). Thus, $\mathcal{R}_{0, i^\star, j^\star} > 1$ is sufficient condition for existence of the endemic equilibrium $\mathcal{E}^\star_{i^\star, j^\star}$.

We can consider the expression mentioned above for the general case of the lattice system (2.2), i.e., when considering diffusion. In this case we have the "lattice" of the basic reproduction numbers $\mathcal{R}_{0, i, j}$, $i, j = \overline{1, N}$ satisfying to

$$\mathcal{R}_{0, i, j} := \frac{V^0_{i, j}}{V^\star_{i, j}}, \qquad i, j = \overline{1, N}, \tag{3.3}$$

where $\mathcal{E}^0_{i, j}$, $i, j = \overline{1, N}$ are nonidentical steady states, which are found as a result of solution of the algebraic system

$$\left(\beta - \delta_v V^0_{i, j}\right) V^0_{i, j} + \hat{S}\left\{V^0_{i, j}\right\} = 0, \qquad i, j = \overline{1, N}, \tag{3.4}$$

endemic states $\mathcal{E}^\star_{i, j} = \left(V^\star_{i, j}, F^\star_{i, j}\right)$, $i, j = \overline{1, N}$ are found using (3.1).

It is worth to say that due to the common theory the conditions $\mathcal{R}_{0, i, j} > 1$, $i, j = \overline{1, N}$ are sufficient for the existence of endemic state $\mathcal{E}^\star_{i, j}$. We will check it only in the Section 4 with help of numerical simulations.

3.3 Local asymptotic stability

In this subsection we discuss the local asymptotic stability of the positive equilibrium $\mathcal{E}^*_{i, j} = \left(V^*_{i, j}, F^*_{i, j}\right)$, $i, j = \overline{1, N}$.

Linearising system (2.2) at $\mathcal{E}^*_{i, j}$, $i, j = \overline{1, N}$, we obtain for $v_{i, j}(t) = V_{i, j}(t) - V^*_{i, j}$ and $f_{i, j}(t) = F_{i, j}(t) - F^*_{i, j}$

$$\begin{cases} \dfrac{dv_{i, j}(t)}{dt} = -\left(\dfrac{\hat{S}\{V^*_{i, j}\}}{V^*_{i, j}} + k(i, j)Dn\right) v_{i, j}(t) - \delta_v V^*_{i, j} v_{i, j}(t - \tau) \\ \qquad\qquad - \gamma V^*_{i, j} f_{i, j}(t - \tau) + \hat{\hat{S}}(i, j, t), \\ \dfrac{df_{i, j}(t)}{dt} = \eta\gamma F^* v_{i, j}(t - \tau) - \delta_f F^*_{i, j} f_{i, j}(t), \end{cases} \qquad i, j = \overline{1, N}. \tag{3.5}$$

where $\hat{S}(i,j,t) = \hat{S}\{V_{i,j}(t)\} + k(i,j)DnV_{i,j}(t)$. We note that the locally uniformly asymptotic stability of the endemic equilibrium $\mathcal{E}_{i,j}^* = \left(V_{i,j}^*, F_{i,j}^*\right)$, $i,j = \overline{1,N}$ of system (2.2) follows from that of the zero solution of system (3.5) (see [30], Theorem 4.2, page 26).

Theorem 3.1. *Assume that:*

1. *The basic reproduction numbers satisfy*

$$\mathcal{R}_{0,i,j} > 1, \qquad i,j = \overline{1,N}, \tag{3.6}$$

2. *The value of time delay τ is less than $\tau^\star$. Here $\tau^\star = \min\{\tau_1, \tau_2\}$, where*

$$\tau_1 := \min_{i,j \in \overline{1,N}} \left[\frac{2K_1(i,j) - k(i,j)D^2 - 1}{\gamma V_{i,j}^* \left[\left(\frac{\delta_v}{\gamma} + 1 \right) k(i,j)D^2 + \left(\frac{2\delta_v}{\gamma} + 1 \right) K_1(i,j) + \delta_v V_{i,j}^* + \frac{\delta_v}{\gamma} + (2\eta\gamma + \delta_f) F_{i,j}^* \right]} \right] > 0, \tag{3.7}$$

$$\tau_2 := \min_{i,j \in \overline{1,N}} \left[\frac{2\delta_f}{K_1(i,j) + (\delta_v + 2\gamma)V_{i,j}^* + 1 + \delta_f F_{i,j}^*} \right] > 0, \tag{3.8}$$

where $K_1(i,j) := \frac{\hat{S}\{V_{i,j}^*\}}{V_{i,j}^*} + k(i,j)Dn + \delta_v V_{i,j}^*$.

Then the positive equilibrium $\mathcal{E}_{i,j}^* = \left(V_{i,j}^*, F_{i,j}^*\right)$, $i,j = \overline{1,N}$ of system (2.2) is uniformly asymptotically stable.

Proof. The assumption (3.6) enables existence of the endemic steady state $\mathcal{E}_{i,j}^* = \left(V_{i,j}^*, F_{i,j}^*\right)$, $i,j = \overline{1,N}$.

Let us rewrite equations (2.2) in the following way

$$\frac{d}{dt} \left[v_{i,j}(t) - \delta_v V_{i,j}^* \int_{t-\tau}^t v_{i,j}(s)ds - \gamma V_{i,j}^* \int_{t-\tau}^t f_{i,j}(s)ds \right] = -K_1(i,j)v_{i,j}(t)$$
$$- \gamma V_{i,j}^* f_{i,j}(t) + \hat{S}(i,j,t), \tag{3.9}$$
$$\frac{d}{dt} \left[f_{i,j}(t)\eta\gamma F_{i,j}^* \int_{t-\tau}^t v_{i,j}(s)ds \right] = \eta\gamma F_{i,j}^* v_{i,j}(t) - \delta_f F_{i,j}^* f_{i,j}(t).$$

We will use Lyapunov functional for the entire system (2.2) of the following form[1]

$$W(t) = \sum_{i,j=1}^N \left\{ \frac{1}{\gamma V_{i,j}^*} W_{i,j,1}(t) + \frac{1}{\eta\gamma F_{i,j}^*} W_{i,j,2}(t) \right\}.$$

It summarizes Lyapunov functionals for all pixels $i,j = \overline{1,N}$. Lyapunov functionals $W_{i,j,1}(t)$ are constructed basing on the first equation from (2.2), $W_{i,j,2}(t)$ use the second ones.

Let us define functional $W_{i,j,1}(t) = W_{i,j,1,1}(t) + W_{i,j,1,2}(t)$, where

$$W_{i,j,1,1}(t) = \left[v_{i,j}(t) - \delta_v V_{i,j}^* \int_{t-\tau}^t v_{i,j}(s)ds - \gamma V_{i,j}^* \int_{t-\tau}^t f_{i,j}(s)ds \right]^2,$$

---

[1] Note that we denote the value of functional $W : \mathbb{C}[-\tau, 0) \to \mathbb{R}^+$, which is calculated at vector-interval $x(t+s)$, $s \in [\tau, 0]$, by $W(t)$ (or sometimes $W(x(t))$).

and

$$W_{i,j,1,2}(t) = \left(\delta_v V_{i,j}^* K_1(i,j) + \delta_v \gamma (V_{i,j}^*)^2 + \delta_v V_{i,j}^* \right) \int_{t-\tau}^{t} \int_{s}^{t} v_{i,j}^2(\xi) d\xi ds$$

$$+ \left(\gamma V_{i,j}^* K_1(i,j) + \gamma^2 (V_{i,j}^*)^2 + \gamma V_{i,j}^* \right) \int_{t-\tau}^{t} \int_{s}^{t} f_{i,j}^2(\xi) d\xi ds$$

Such form of $W_{i,j,1,1}(t)$ allows us to use the first equation of (3.9) for getting derivative. Lyapunov functionals $W_{i,j,1,2}(t)$ are chosen in such a form in order to reduce the derivative[2] of $W_{i,j,1}(t)$ to quadratic form of $v_{i,j}(t)$ and $f_{i,j}(t)$ as close as possible.

We define $W_{i,j,2}(t) = W_{i,j,2,1}(t) + W_{i,j,2,2}(t)$. Considering the second equation of (3.9) we define

$$W_{i,j,2,1}(t) = \left[f_{i,j}(t) + \eta \gamma F_{i,j}^* \int_{t-\tau}^{t} v_{i,j}(s) ds \right]^2.$$

$W_{i,j,2,2}(t)$ is defined in the following form

$$W_{i,j,2,2}(t) = \eta \gamma F_{i,j}^* (\eta \gamma F_{i,j}^* + F_{i,j}^* \delta_f) \int_{t-\tau}^{t} \int_{t-\tau}^{t} v_{i,j}^2(\xi) d\xi ds, \qquad (3.10)$$

allowing to reduce the derivative of $W_{i,j,2}(t)$ to quadratic form of $v_{i,j}(t)$ and $f_{i,j}(t)$.

Further let us find derivatives of Lyapunov functionals and estimate them comparing with some quadratic form of $v_{i,j}(t)$ and $f_{i,j}(t)$.

Calculating the derivative of $W_{i,j,1,1}$ along solutions of (3.9), we have

$$\frac{dW_{i,j,1,1}(t)}{dt} = 2 \left[v_{i,j}(t) - \delta_v V_{i,j}^* \int_{t-\tau}^{t} v_{i,j}(s) ds - \gamma V_{i,j}^* \int_{t-\tau}^{t} f_{i,j}(s) ds \right]$$

$$\times \left[-K_1(i,j) v_{i,j}(t) - \gamma V_{i,j}^* f_{i,j}(t) + \hat{\hat{S}}(i,j,t) \right]$$

Using the inequality $2ab \leq a^2 + b^2$, we get

$$\frac{dW_{i,j,1,1}(t)}{dt}$$

$$\leq -2K_1(i,j) v_{i,j}^2(t) - 2\gamma V_{i,j}^* v_{i,j}(t) f_{i,j}(t)$$

$$+ 2\delta_v V_{i,j}^* K_1(i,j) \int_{t-\tau}^{t} |v_{i,j}(s)| |v_{i,j}(t)| ds + 2\gamma V_{i,j}^* K_1(i,j) \int_{t-\tau}^{t} |f_{i,j}(s)| |v_{i,j}(t)| ds$$

$$+ 2\delta_v \gamma (V_{i,j}^*)^2 \int_{t-\tau}^{t} |v_{i,j}(s)| |f_{i,j}(t)| ds + 2\gamma^2 (V_{i,j}^*)^2$$

$$\times \int_{t-\tau}^{t} |f_{i,j}(s)| |f_{i,j}(t)| ds + 2v_{i,j}(s) \hat{\hat{S}}\{i,j,t\}$$

$$+ 2\delta_v V_{i,j}^* \int_{t-\tau}^{t} |v_{i,j}(s)| |\hat{\hat{S}}\{i,j,t\}| ds + 2\gamma V_{i,j}^* \int_{t-\tau}^{t} |f_{i,j}(s)| |\hat{\hat{S}}\{i,j,t\}| ds$$

---

[2] Note, that in general this derivative may not exist for delayed differential equations. To avoid this difficulty, R. D. Driver [14] offered a "constructive" definition of a quantity which will always exist and which will play the role of a derivative in delayed differential equations. Namely, it is the upper right-hand-side derivative. Due to the definition [14] (page 414) the upper right-hand-side derivative of a locally Lipschitz continuous function $W : \mathbb{R}^N \to \mathbb{R}^+$ along trajectory $x(\cdot)$ is defined by $D^+W = \limsup_{\Delta t \to 0^+} \frac{W(x(t+\Delta t)) - W(x(t))}{\Delta t}$. Hereinafter, for simplicity we call the upper right-hand-side derivative of Lyapunov functional as the derivative of Lyapunov functional.

$$\leq -2K_1(i,j)v_{i,j}^2(t) - 2\gamma V_{i,j}^* v_{i,j}(t)f_{i,j}(t) + \delta_v V_{i,j}^* K_1(i,j)\left[\tau v_{i,j}^2(t) + \int_{t-\tau}^t v_{i,j}^2(s)ds\right]$$

$$+ \gamma V_{i,j}^* K_1(i,j)\left[\tau v_{i,j}^2(t) + \int_{t-\tau}^t f_{i,j}^2(s)ds\right] + \delta_v\gamma(V_{i,j}^*)^2\left[\tau f_{i,j}^2(t) + \int_{t-\tau}^t v_{i,j}^2(s)ds\right]$$

$$+ \gamma^2(V_{i,j}^*)^2\left[\tau f_{i,j}^2(t) + \int_{t-\tau}^t f_{i,j}^2(s)ds\right] + v_{i,j}^2(t) + \hat{\hat{S}}\{i,j,t\}$$

$$+ \delta_v V_{i,j}^*\left[\tau\hat{\hat{S}}\{i,j,t\} + \int_{t-\tau}^t v_{i,j}^2(s)ds\right] + \gamma V_{i,j}^*\left[\tau\hat{\hat{S}}\{i,j,t\} + \int_{t-\tau}^t f_{i,j}^2(s)ds\right] \tag{3.11}$$

Here $\hat{\hat{S}}(i,j,t) := D^2\left[V_{i-1,j}^2(t) + V_{i+1,j}^2(t) + V_{i,j-1}^2(t) + V_{i,j+1}^2(t)\right]$.

Then we derive from (3.11) that

$$\frac{dW_{i,j,1}(t)}{dt} \leq \left(-2K_1(i,j) + 2\delta_v V_{i,j}^* K_1(i,j)\tau + \gamma V_{i,j}^* K_1 i, j\tau + \delta_v\gamma(V_{i,j}^*)^2\tau + 1 + \delta_v V_{i,j}^*\tau\right)v_{i,j}^2$$

$$- 2\gamma V_{i,j}^* v_{i,j}(t)f_{i,j}(t) + \left(\gamma V_{i,j}^* K_1\tau + \delta_v\gamma(V_{i,j}^*)^2\tau + 2\gamma^2(V_{i,j}^*)^2\tau + \gamma V_{i,j}^*\tau\right)f_{i,j}^2 \tag{3.12}$$

$$+ \left(1 + \delta_v V_{i,j}^*\tau + \gamma V_{i,j}^*\tau + \gamma V_{i,j}^*\tau\right)\hat{\hat{S}}\{i,j,t\}.$$

Then, calculating the derivative of $W_{i,j,2,1}(t)$ along solutions of (3.9), we derive that

$$\frac{dW_{i,j,2,1}(t)}{dt} = 2\left[f_{i,j}(t) + \eta\gamma F_{i,j}^*\int_{t-\tau}^t v_{i,j}(s)\right] \times \left[\eta\gamma F_{i,j}^* v_{i,j}(t) - \delta_f F_{i,j}^* f_{i,j}(t)\right]$$

$$\leq 2\eta\gamma F_{i,j}^* v_{i,j}f_{i,j}(t) - 2\delta_f F_{i,j}^* f_{i,j}^2(t) + 2(\eta\gamma F_{i,j}^*)^2\int_{t-\tau}^t |v_{i,j}(s)||v_{i,j}(t)|ds$$

$$+ 2\eta\gamma(F_{i,j}^*)^2\delta_f\int_{t-\tau}^t |v_{i,j}(s)||f_{i,j}(t)|ds \tag{3.13}$$

$$\leq 2\eta\gamma F_{i,j}^* v_{i,j}f_{i,j}(t) - 2\delta_f F_{i,j}^* f_{i,j}^2(t) + (\eta\gamma F_{i,j}^*)^2\left[\tau v_{i,j}^2(t) + \int_{t-\tau}^t v_{i,j}^2(s)ds\right]$$

$$+ \eta\gamma(F_{i,j}^*)^2\delta_f\left[\tau f_{i,j}^2(t) + \int_{t-\tau}^t v_{i,j}^2(s)ds\right]$$

It follows from (3.13) and (3.10) that

$$\frac{dW_{i,j,2}(t)}{dt} \leq 2\eta\gamma F_{i,j}^* v_{i,j}(t)f_{i,j}(t) - (2\delta_f F_{i,j}^* - \eta\gamma(F_{i,j}^*)^2\delta_f\tau)f_{i,j}^2(t)$$

$$+ (2(\eta\gamma F_{i,j}^*)^2\tau + \eta\gamma(F_{i,j}^*)^2\tau)v_{i,j}^2(t). \tag{3.14}$$

Finally, calculating the derivative of $W(t)$ along solutions of (3.9) and rearranging counterparts $D^2 v_{i,j}^2(t)$, we have[3]

---

[3]Here we take into account the fact that as a result of interconnection we have additional value $4Dv_{i,j}^2(t)$ "flowing" into pixel (i,j) from two-three-four neighboring pixels: two pixels for pixels $(1,1)$, $(N,1)$, (N,N), $(1,N)$, three pixels for pixels $(1,j)$, $j = \overline{2,N-1}$, $(i,1)$, $i = \overline{2,N-1}$, (N,j), $j = \overline{2,N-1}$, (i,N), $i = \overline{2,N-1}$ and four pixels due to figure 2.1 for the rest "internal" pixels.

$$\frac{dW(t)}{dt} \leq \sum_{i,j=1}^{N} \left\{ \left[\frac{1}{\gamma V_{i,j}^*} \left(-2K_1(i,j) + 2\delta_v V_{i,j}^* K_1(i,j)\tau + \gamma V_{i,j}^* K_1(i,j)\tau + \delta_v \gamma (V_{i,j}^*)^2 \tau + 1 + \delta_v V_{i,j}^* \tau \right) \right. \right.$$

$$\left. + \frac{1}{\eta \gamma F_{i,j}^*} \left(2(\eta \gamma F_{i,j}^*)^2 \tau + \eta \gamma (F_{i,j}^*)^2 \delta_f \tau \right) \right] v_{i,j}^2(t)$$

$$+ \left[\frac{1}{\gamma V_{i,j}^*} \left(\gamma V_{i,j}^* K_1(i,j)\tau + \delta_v \gamma (V_{i,j}^*)^2 \tau + 2\gamma^2 (V_{i,j}^*)^2 \tau + \gamma V_{i,j}^* \tau \right) \right.$$

$$\left. + \frac{1}{\eta \gamma F_{i,j}^*} \left(-2\delta_f F_{i,j}^* + \eta \gamma (F_{i,j}^*)^2 \delta_f \tau \right) \right] f_{i,j}^2(t)$$

$$\left. + \frac{1}{\gamma V_{i,j}^*} (1 + \delta_v V_{i,j}^* \tau + \gamma V_{i,j}^* \tau) \hat{\hat{S}}\{i,j,t\} \right\}$$

$$= \sum_{i,j=1}^{N} \left\{ \left[\frac{1}{\gamma V_{i,j}^*} \left(-2K_1(i,j) + k(i,j)D^2(1 + \delta_v V_{i,j}^* \tau + \gamma V_{i,j}^* \tau) + 2\delta_v V_{i,j}^* K_1(i,j)\tau \right. \right. \right.$$

$$\left. + \gamma V_{i,j}^* K_1(i,j)\tau + \delta_v \gamma (V_{i,j}^*)^2 \tau + 1 + \delta_v V_{i,j}^* \tau \right)$$

$$+ \frac{1}{\eta \gamma F_{i,j}^*} \left(2(\eta \gamma F_{i,j}^*)^2 \tau + \eta \gamma (F_{i,j}^*)^2 \delta_f \tau \right) \right] v_{i,j}^2(t)$$

$$+ \left[\frac{1}{\gamma V_{i,j}^*} \left(\gamma V_{i,j}^* K_1(i,j)\tau + \delta_v \gamma (V_{i,j}^*)^2 \tau + 2\gamma^2 (V_{i,j}^*)^2 \tau + \gamma V_{i,j}^* \tau \right) \right.$$

$$\left. + \frac{1}{\eta \gamma F_{i,j}^*} \left(-2\delta_f F_{i,j}^* + \eta \gamma (F_{i,j}^*)^2 \delta_f \tau \right) \right] f_{i,j}^2(t) \right\}.$$

Applying the assumption $\tau < \tau^\star$ we get

$$\frac{dW(t)}{dt} \leq \sum_{i,j=1}^{N} \left\{ \left[\frac{1}{\gamma V_{i,j}^*} \left(-2K_1(i,j) + k(i,j)D^2(1 + \delta_v V_{i,j}^* \tau_1 + \gamma V_{i,j}^* \tau_1) + 2\delta_v V_{i,j}^* K_1(i,j)\tau_1 \right. \right. \right.$$

$$\left. + \gamma V_{i,j}^* K_1(i,j)\tau_1 + \delta_v \gamma (V_{i,j}^*)^2 \tau_1 + 1 + \delta_v V_{i,j}^* \tau_1 \right)$$

$$+ \frac{1}{\eta \gamma F_{i,j}^*} \left(2(\eta \gamma F_{i,j}^*)^2 \tau_1 + \eta \gamma (F_{i,j}^*)^2 \delta_f \tau_1 \right) \right] v_{i,j}^2(t)$$

$$+ \left[\frac{1}{\gamma V_{i,j}^*} \left(\gamma V_{i,j}^* K_1(i,j)\tau_2 + \delta_v \gamma (V_{i,j}^*)^2 \tau_2 + 2\gamma^2 (V_{i,j}^*)^2 \tau_2 + \gamma V_{i,j}^* \tau_2 \right) \right.$$

$$\left. + \frac{1}{\eta \gamma F_{i,j}^*} \left(-2\delta_f F_{i,j}^* + \eta \gamma (F_{i,j}^*)^2 \delta_f \tau_2 \right) \right] f_{i,j}^2(t) \right\}.$$

After substitution of estimates of τ_1 and τ_2 due to (3.7), (3.8), we can see that there are negative constants $\alpha_{1,i,j}, \alpha_{2,i,j} < 0$, $i,j = \overline{1,N}$ such that

$$\frac{dW(t)}{dt} \leq \sum_{i,j=1}^{N} \left\{ \alpha_{1,i,j} v_{i,j}^2(t) + \alpha_{2,i,j} f_{i,j}^2(t) \right\}.$$

$V_{i,j}^0$	1	2	3	4
1	5.951989	7.420163	7.659892	5.966077
2	5.907517	6.180657	6.183041	5.718244
3	5.703791	5.772168	5.737166	5.500841
4	5.322284	5.459773	5.440191	5.254434

Table 4.1: The values of $V_{i,j}^0$, $i,j = \overline{1,4}$.

$V_{i,j}^\star$	1	2	3	4
1	1.8491747	2.1662985	2.2047148	1.8500473
2	1.8628235	1.9105332	1.9105342	1.8289965
3	1.8445217	1.8573021	1.8527207	1.8092236
4	1.7757109	1.8073319	1.8056241	1.7683109

Table 4.2: The values of $V_{i,j}^\star$, $i,j = \overline{1,4}$.

$\square$

Corollary 3.2. *Assume that the conditions* (3.6) *of Theorem* 3.1 *are true. Then positive equilibrium state* $\mathcal{E}_{i,j}^* = (V^*, F^*)$, $i,j = \overline{1,N}$ *of system* (2.2) *is locally asymptotic stable if*

$$\alpha_1 := \max_{i,j \in \overline{1,N}} \left[\frac{1}{\gamma V_{i,j}^*} (-2K_1(i,j) + k(i,j)D^2(1 + \delta_v V_{i,j}^*\tau + \gamma V_{i,j}^*\tau) \right.$$
$$+ 2\delta_v V_{i,j}^* K_1(i,j)\tau + \gamma V_{i,j}^* K_1(i,j)\tau + \delta_v \gamma (V_{i,j}^*)^2\tau + 1 + \delta_v V_{i,j}^*\tau)$$
$$\left. + 2\eta\gamma F_{i,j}^*\tau + F_{i,j}^\star \delta_f \tau \right] < 0,$$

$$\alpha_2 := \max_{i,j \in \overline{1,N}} \left[K_1(i,j)\tau + \delta_v V_{i,j}^*\tau + 2\gamma V_{i,j}^*\tau + \tau + \frac{1}{\eta\gamma}(-2\delta_f + \eta\gamma F_{i,j}^*\delta_f\tau) \right] < 0,$$

Remark 3.3. Conditions of local asymptotic stability of positive equilibrium state $\mathcal{E}_{i,j}^* = (V_{i,j}^*, F_{i,j}^*)$, $i,j = \overline{1,N}$ of system (2.2) are dependent on diffusion D and factor n also.

4 Numerical simulations

We consider model (2.2) at $N = 4$, $\beta = 2\,\text{min}^{-1}$, $\gamma = 2\frac{mL}{\text{min}\cdot\mu g}$, $\mu_f = 1\,\text{min}^{-1}$, $\eta = 0.8/\gamma$, $\delta_v = 0.5\frac{mL}{\text{min}\cdot\mu g}$, $\delta_f = 0.5\frac{mL}{\text{min}\cdot\mu g}$, $D = 2.22\,\text{min}^{-1}$.

4.1 Numerical simulation of 4×4 pixels array

First of we calculate the basic reproductive numbers $\mathcal{R}_{0,i,j}$, $i,j = \overline{1,4}$. Solving (3.4) we have the values of equilibrium without antibodies $V_{i,j}^0$, $i,j = \overline{1,4}$ (see Table 4.1).

The values of $V_{i,j}^\star$, $i,j = \overline{1,4}$ for the endemic steady state are presented in the Table 4.2. Hence, the basic reproductive numbers which are calculated due to (3.3) are shown in the Table 4.3. We see that the conditions (3.6) hold. Thus, equilibrium without antibodies $\mathcal{E}_{i,j}^0$,

$R^\star_{0,i,j}$	1	2	3	4
1	3.218727	3.425273	3.474323	3.224824
2	3.171270	3.235043	3.236289	3.126438
3	3.092287	3.107824	3.096617	3.040443
4	2.997269	3.020902	3.012915	2.971442

Table 4.3: The values of $R_{0,i,j}$, $i,j = \overline{1,4}$.

$i,j = \overline{1,4}$ is unstable and there exists endemic equilibrium $\mathcal{E}^\star_{i,j}$, $i,j = \overline{1,4}$.

The following numerical simulations were implemented at different values of $n \in (0,1]$. For example, at $n = 0.9$ corresponding simulations for $\tau > 0$ (min) are presented (see Figs. 4.1, 4.2, 4.3, 4.4)

Here we can see that when changing the value of τ we have changes of qualitative behavior of pixels and entire immunosensor. We considered the parameter value set given above and computed the long-time behavior of the system (2.2) for $\tau = 0.05, 0.22, 0.23$, 0.2865, and 0.28725. The phase diagrams of the antibody vs. antigen populations for the pixel $(1,1)$ for these values of τ are shown in Figs. 4.1, 4.2, 4.3, 4.4, 4.5.

For example, at $\tau \in [0,0.22]$ we can see trajectories corresponding to stable node for all pixels (see Figs. 4.1, 4.2). At values τ near 0.2223 min Hopf bifurcation occurs and further trajectories correspond to stable limit cycles of ellipsoidal form for all pixels (see Fig. 4.3 for $\tau = 0.23$). We note that in order that the numerical solutions regarding Hopf bifurcation were in agreement with the theoretical results, we should look for a complex conjugate pair of purely imaginary solutions of the corresponding characteristic equation of the linearized system (3.5).

For $\tau = 0.23$, the phase diagrams in Fig. 4.3 show that the solution is a limit cycle with two local extrema (one local maximum and one local minimum) per cycle. Then for $\tau = 0.2825$ the solution is a limit cycle with four local extrema per cycle, and, for $\tau = 0.2868, 0.2869, 0.28695$ the solutions are limit cycles with 8, 16 and 32 local extrema per cycle, respectively. Finally, for $\tau = 0.28725$, the behavior shown in Figs. 4.5 is obtained which looks like chaotic behavior. In this paper, we have regarded behavior as "chaotic" if no periodic behavior could be found in the long-time behavior of the solutions.

As a check that the solution is chaotic for $\tau = 0.28725$, we perturbed the initial conditions to test the sensitivity of the system. Fig. 4.6 shows a comparison of the solutions for the antigen population $V_{1,3}$ with initial conditions $V_{1,3}(t) = 1$ and $V_{1,3}(t) = 1.001$, $t \in [-\tau, 0]$, and identical all the rest ones. Near the initial time the two solutions appear to be the same, but as time increases there is a marked difference between the solutions supporting the conclusion that the system behavior is chaotic at $\tau = 0.28725$.

We have also checked numerically that the solutions for the limit cycles are periodic and computed the periods for each of the local maxima and minima in the cycles. Fig. 4.7 shows a plot of the number of local minima and maxima in limit cycles of the $V_{1,3}$ as τ increases from 0 to 0.28725. In the chaotic solution region, the numerical calculations (not shown in this paper) confirmed that no periodic behavior could be found.

A bifurcation diagram showing the maximum and minimum points for the limit cycles for the antigen population $V_{1,3}$ as a function of time delay is given in Fig. 4.7. The Hopf bifurcation from the stable equilibrium point to a simple limit cycle and the sharp transitions at critical values of the time delay between limit cycles with increasing numbers of maximum and minimum points per cycle can be clearly seen.
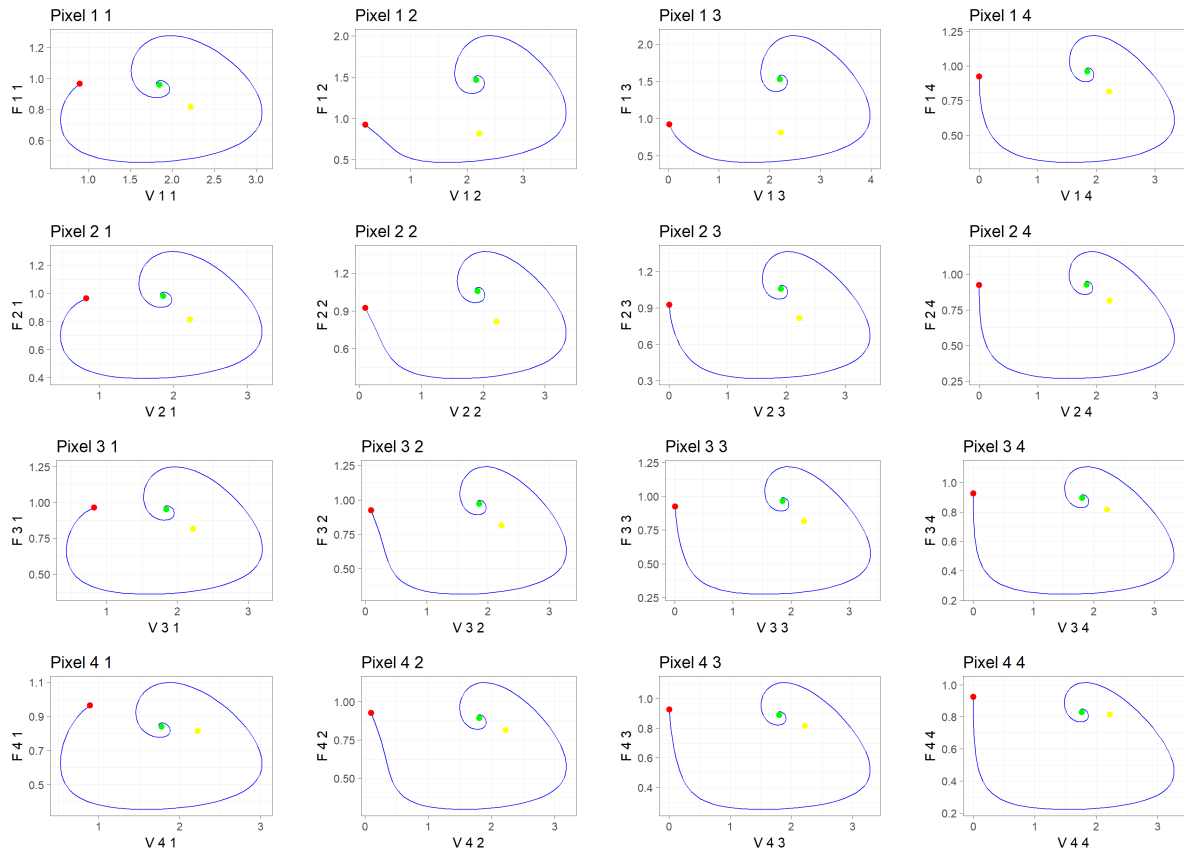
Figure 4.1: The phase planes of the system (2.2) for antibody populations $F_{i,j}$ versus antigen populations $V_{i,j}$, $i, j = \overline{1,4}$. Numerical simulation of the system (2.2) at $n = 0.9$, $\tau = 0.05$. Here ● indicates initial state, ● indicates identical steady state, ● indicates nonidentical steady state. The solution converges to the nonidentical steady state which is stable focus when $\tau = 0.05 < \tau_0 \approx 0.2223$.
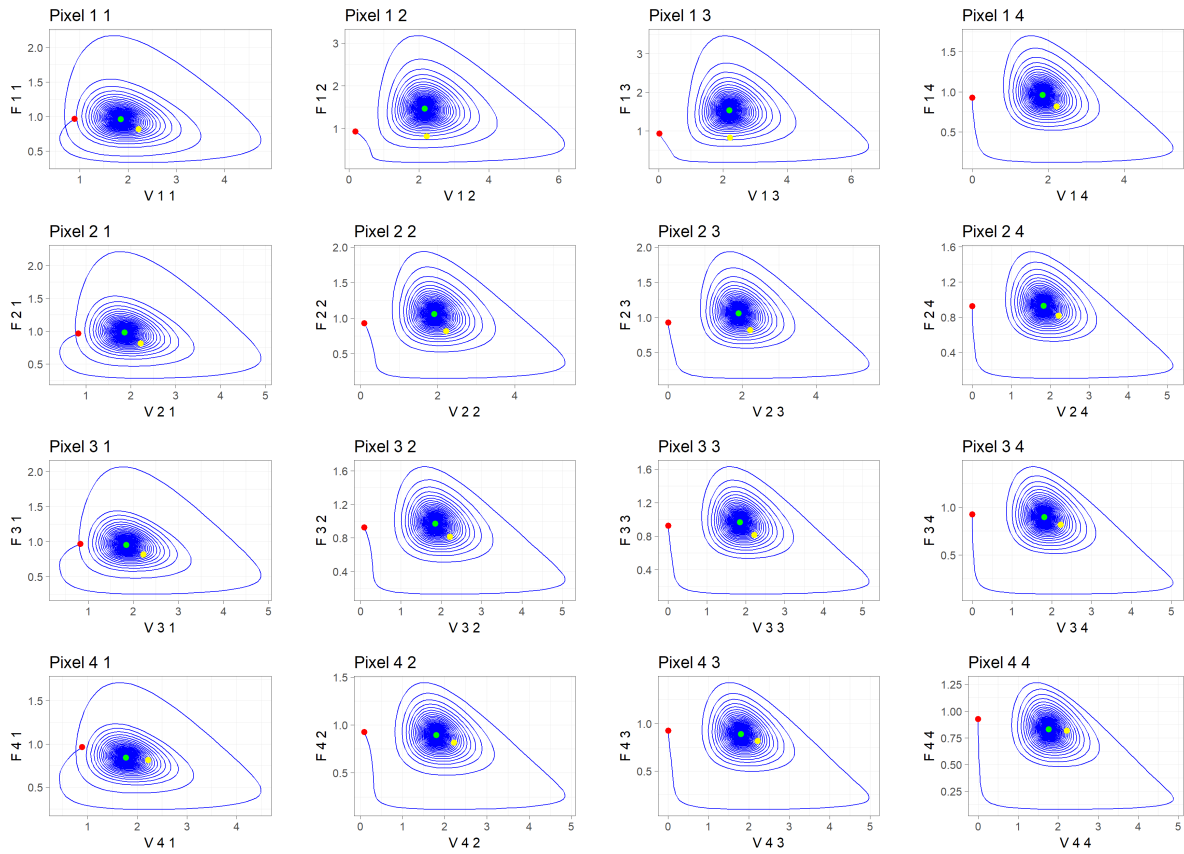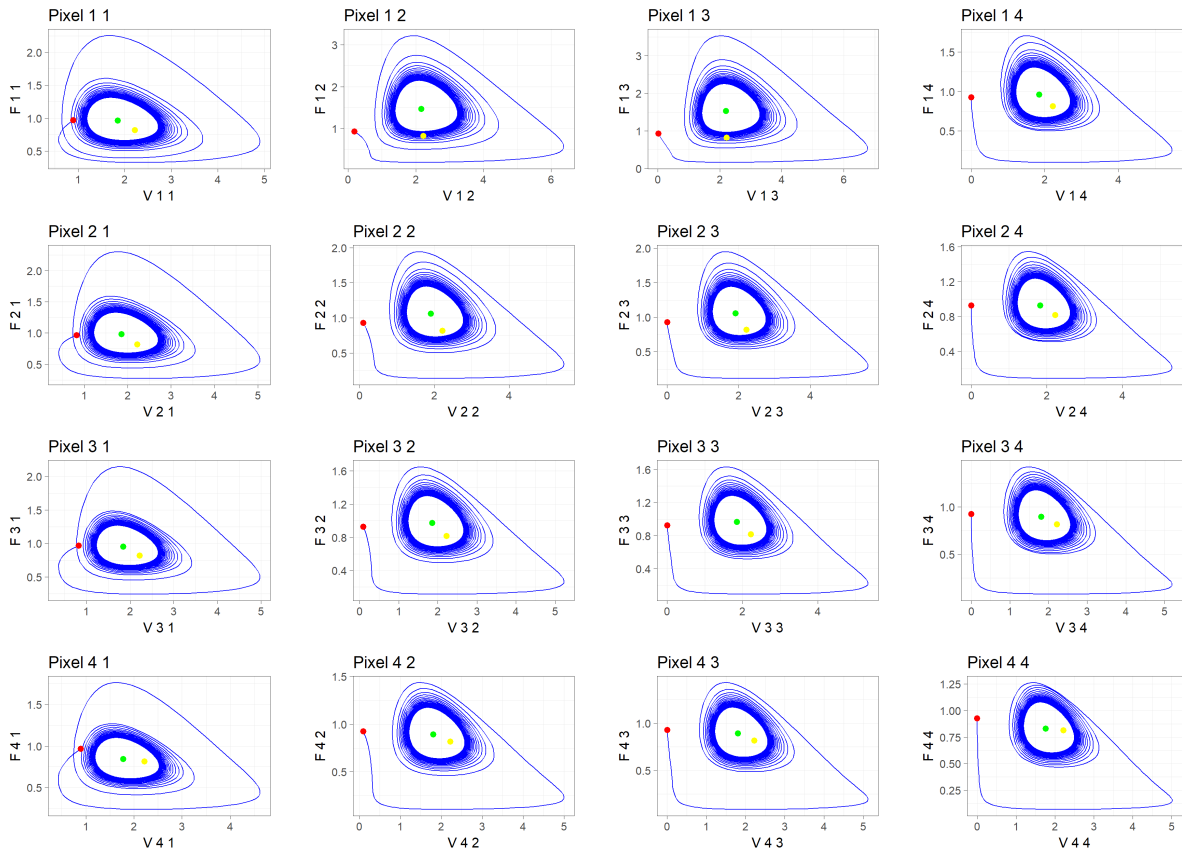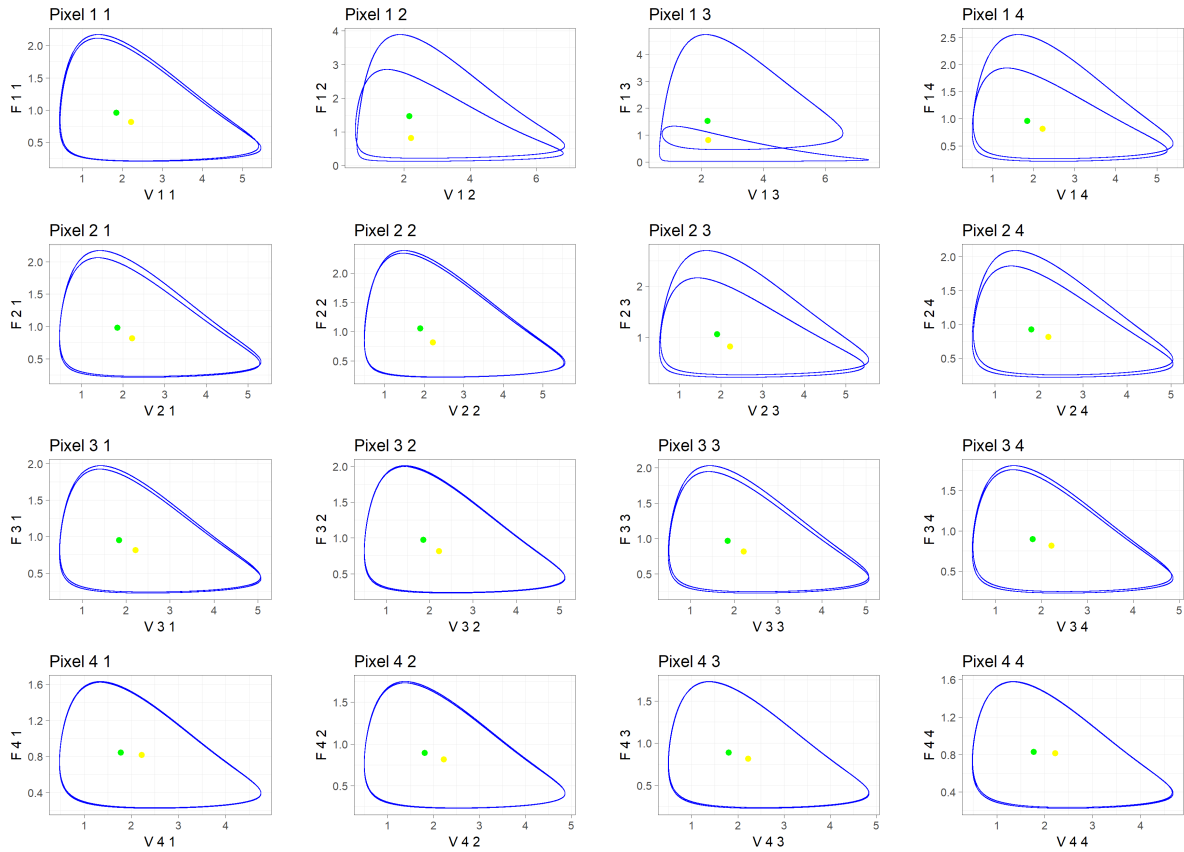
Figure 4.2: The phase plane plots of the system (2.2) for antibody populations $F_{i,j}$ versus antigen populations $V_{i,j}$, $i, j = \overline{1,4}$. Numerical simulation of the system (2.2) at $n = 0.9$, $\tau = 0.22$. Here • indicates initial state, • indicates identical steady state, • indicates nonidentical steady state. The solution converges to the nonidentical steady state which is stable focus when $\tau = 0.22 < \tau_0 \approx 0.2223$.
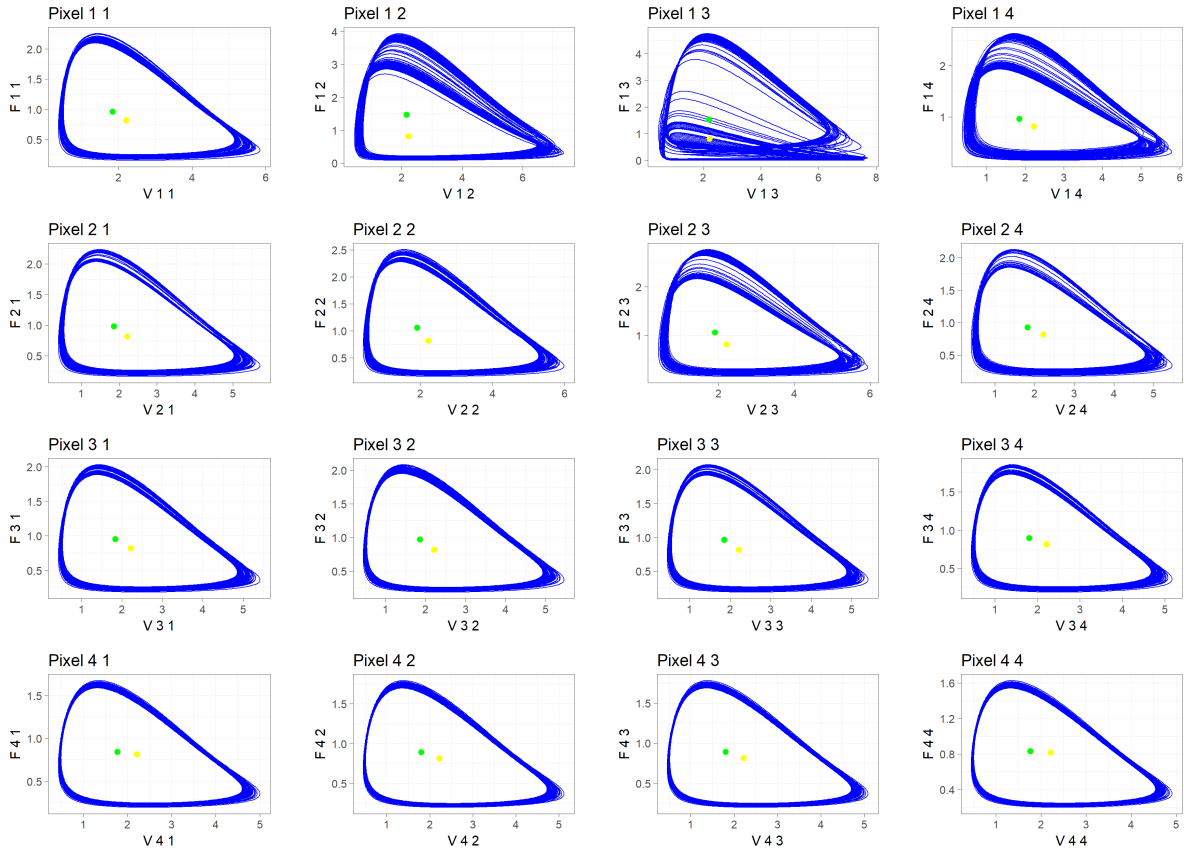
Figure 4.3: The phase planes of the system (2.2) for antibody populations $F_{i,j}$ versus antigen populations $V_{i,j}$, $i, j = \overline{1, 4}$. Numerical simulation of the system (2.2) at $n = 0.9$, $\tau = 0.23$. Here ● indicates initial state, ● indicates identical steady state, ● indicates nonidentical steady state. The solution converges to a stable limit cycle.

Figure 4.4: The limit cycles on the phase plane plots of the system (2.2) for antibody populations $F_{i,j}$ versus antigen populations $V_{i,j}$, $i,j = \overline{1,4}$. Numerical simulation of the system (2.2) at $n = 0.9$, $\tau = 0.2865$. Here ● indicates identical steady state, ● indicates nonidentical steady state. Limit cycles are obtained as trajectories for $t \in [550, 800]$. The solution converges to a stable limit cycle with four local extrema per cycle.

Figure 4.5: The phase plane plots of the system (2.2) for antibody populations $F_{i,j}$ versus antigen populations $V_{i,j}$, $i,j = \overline{1,4}$. Numerical simulation of the system (2.2) at $n = 0.9$, $\tau = 0.28725$. Here ● indicates identical steady state, ● indicates nonidentical steady state. Trajectories are constructed for $t \in [550, 800]$. The solution behavior looks chaotic.
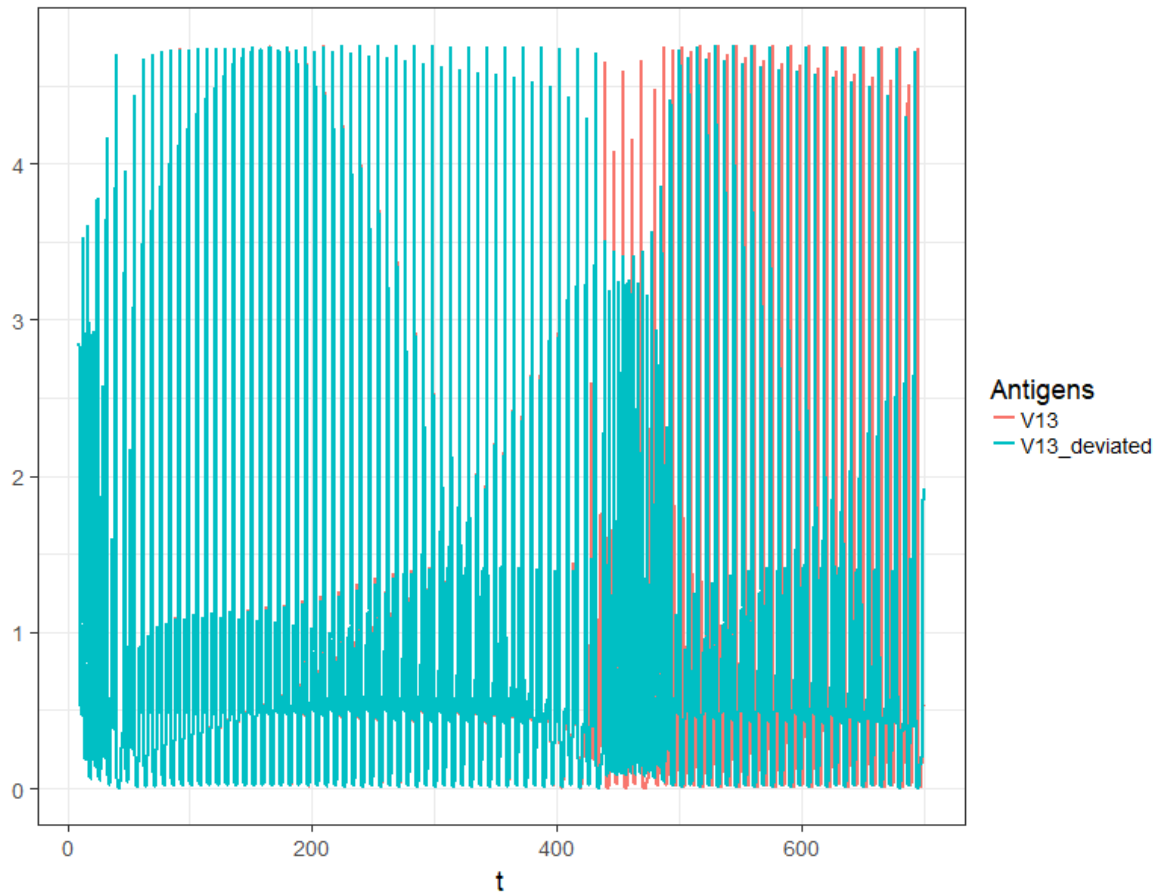
Figure 4.6: The time series of the solutions to the system 2.2 for the antigen population $V_{1,3}$ from $t = 0$ to 700 with $\tau = 0.28725$ for initial conditions $V_{1,3}(t) = 1$ and $V_{1,3}(t) = 1.001$ (deviated), $t \in [-\tau, 0]$, and identical all the rest ones. At the beginning the two solutions appear to be the same, but as time increases there is a marked difference between the solutions supporting the conclusion that the system behavior is chaotic.
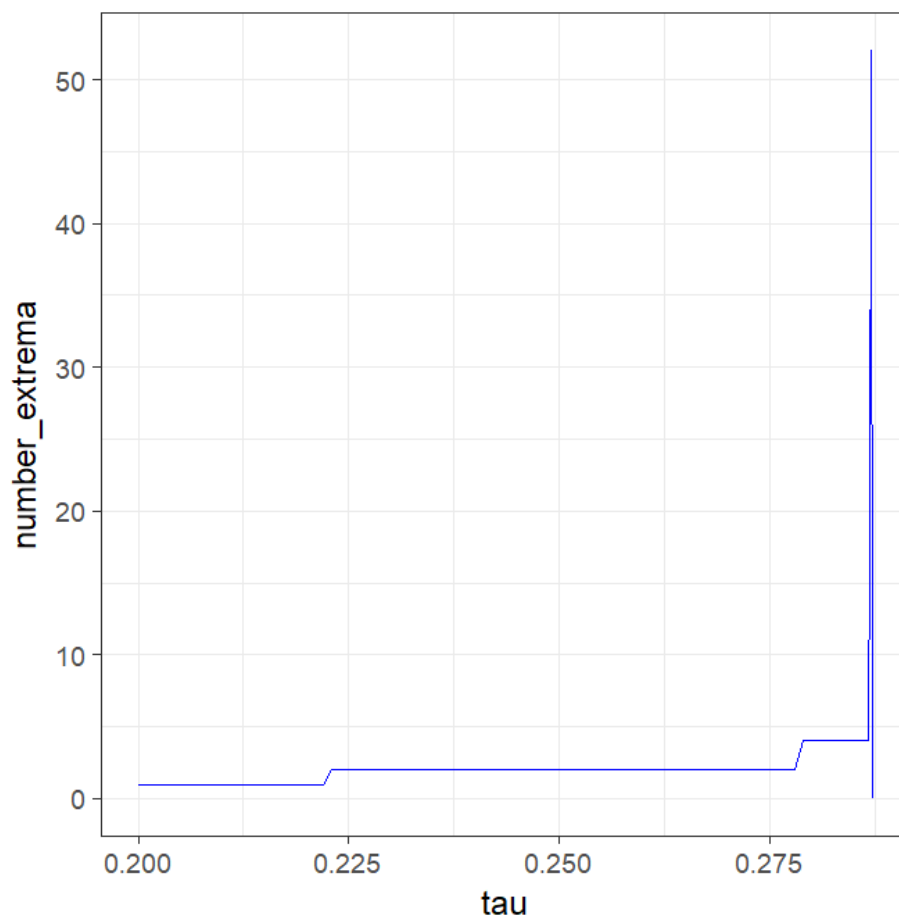
Figure 4.7: Number of local extrema per cycle. No periodic behavior could be found at $\tau \approx 0.28725$.
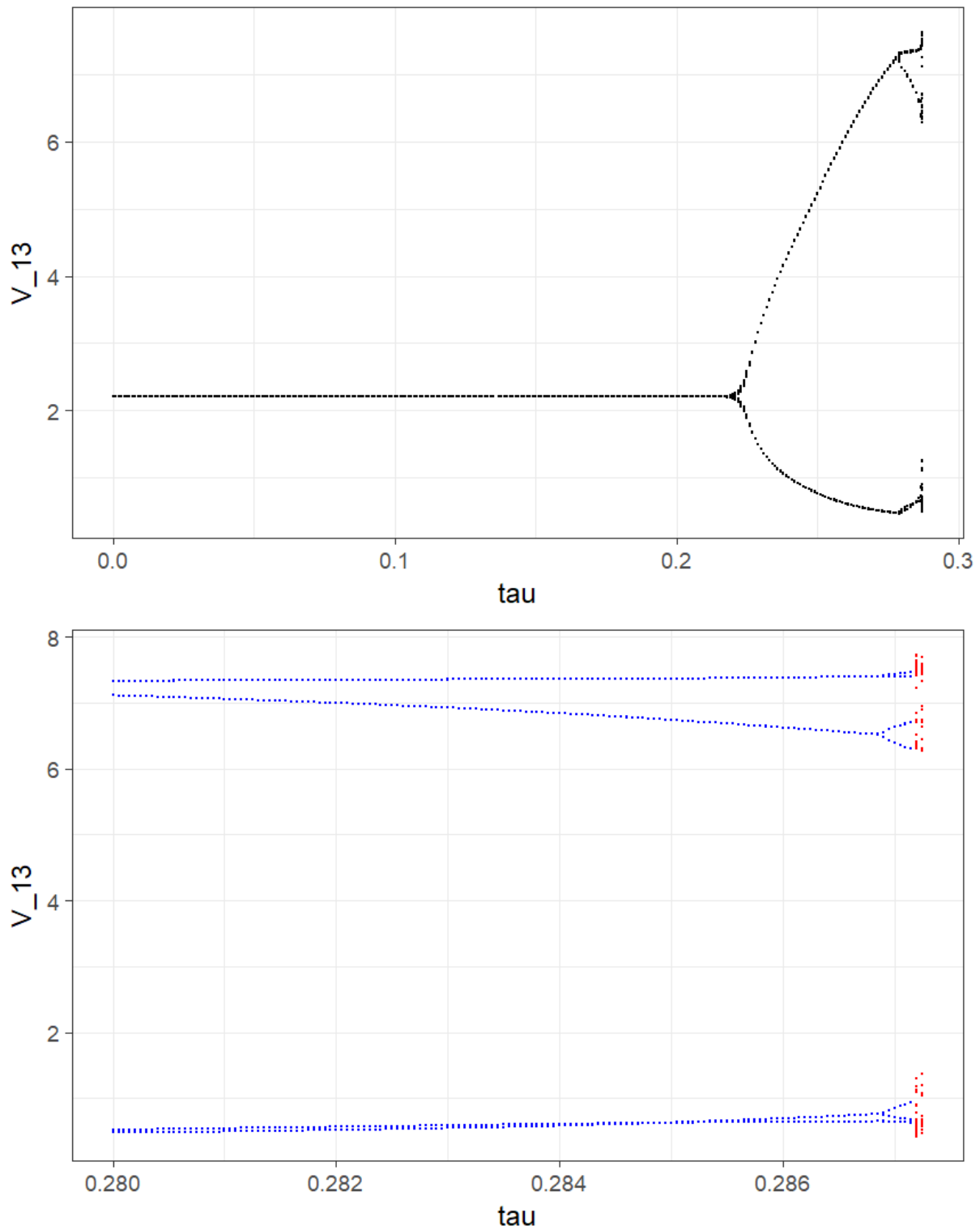
Figure 4.8: A bifurcation diagram showing the "bifurcation path to chaos" as the time delay is increased. The points show the local extreme points per cycle for the $V_{1,3}$ population. Chaotic-type solutions occur at $\tau \approx 0.28725$ and are indicated in red in the figure with value 0 for the number of extreme points.

$\tau^\star$	0.05	0.22	0.23	0.2865
α_1	-2.037159	1.300445	1.496775	1.357042
α_2	-0.3894881	2.536252	2.708355	3.284341

Table 4.4: The values of $\tau^\star$, α_1 and α_2 which are calculated based on the Theorem 3.1 and Corollary 3.2 for $N = 4$.

$\tau^\star$	0.05	0.22	0.23	0.2865
α_1	-2.927095	0.9655621	1.194542	2.488278
α_2	-0.2742058	3.043494	3.238653	4.341301

Table 4.5: The values of $\tau^\star$, α_1 and α_2 which are calculated based on the Theorem 3.1 and Corollary 3.2 for $N = 16$.

When checking conditions of the Theorem 3.1 we obtained that they are satisfied for the values $\tau \leq \tau^\star = 0.05$ (see Table 4.4)

4.2 Numerical simulation of 16 × 16 pixels array

We consider model (2.2) at $N = 16$ and all the rest parameters are as mentioned above. We see that increasing number of pixels affects in "acceleration" of appearance of chaotic behavior. For example, at $n = 0.9$ we have limit cycle at $\tau = 0.23$, $N = 4$. Pay attention that it will be a series of cycle duplication or even chaos at $N = 16$ (see Figs. 4.9, 4.10).

5 Conclusions

In the work we offered model of immunosensor which is based on the system of lattice differential equations with delay. The main result of the work is conditions of local asymptotic stability for endemic state. For this purpose we have used method of Lyapunov functionals. It combines general approach for construction of Lyapunov functionals of predator–prey models with lattice differential equations. As compared with stability conditions which are based on the basic reproduction numbers it allows to estimate the values of delay admitting stability.

Numerical examples showed us influence on stability of different parameters. Increasing time delay we transmit from stable node to limit cycle and finally to chaotic behavior. Disbalance constant $n \in (0, 1]$ also affects on stability characteristics. Decreasing n we narrow interval of asymptotic stability for delay τ. For some values of parameters, we found numerically that the behavior of the system became increasingly complicated as the time delay was increased. In this case, we found that for small delay the system could have a stable steady solution. Then, as the time delay was increased, the stable steady solution changed at a critical value of τ to a stable limit cycle.

However, the numerical simulations showed much more complicated behavior. Then as the time delay was increased, the behavior changed from convergence to simple limit cycle to convergence to complicated limit cycles with an increasing number of local maxima and minima per cycle until at sufficiently high time delay the behavior became chaotic. This change in behavior can be called a bifurcation path to chaos. From our analysis and numerical simulations, we have found no evidence that chaos can occur except through variation in the time delay. It would clearly be desirable if some analytical conditions could be found that could
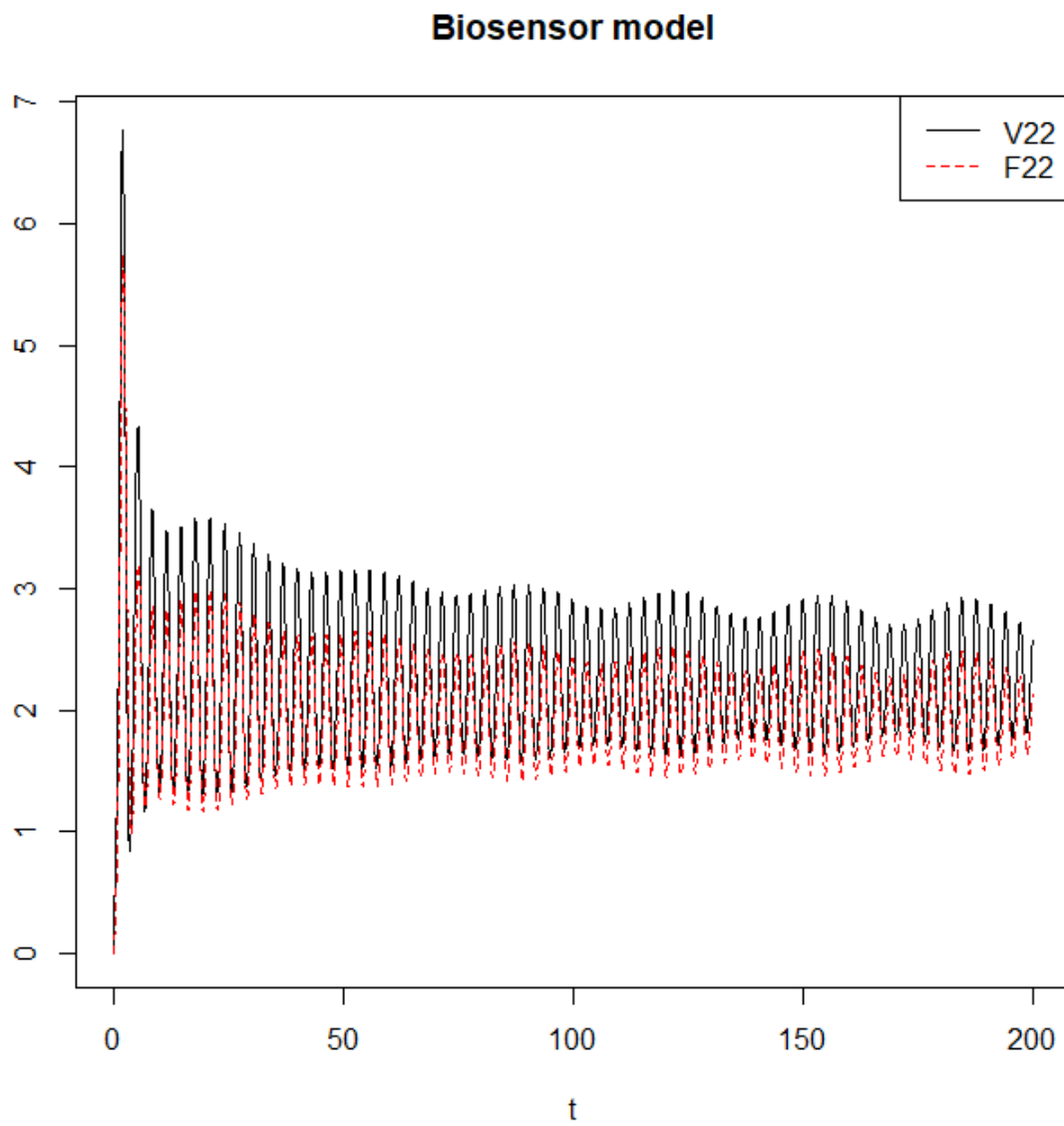
Figure 4.9: Numerical simulation of changes of populations in pixel (2,2) at $N = 16$, $\tau = 0.23$.
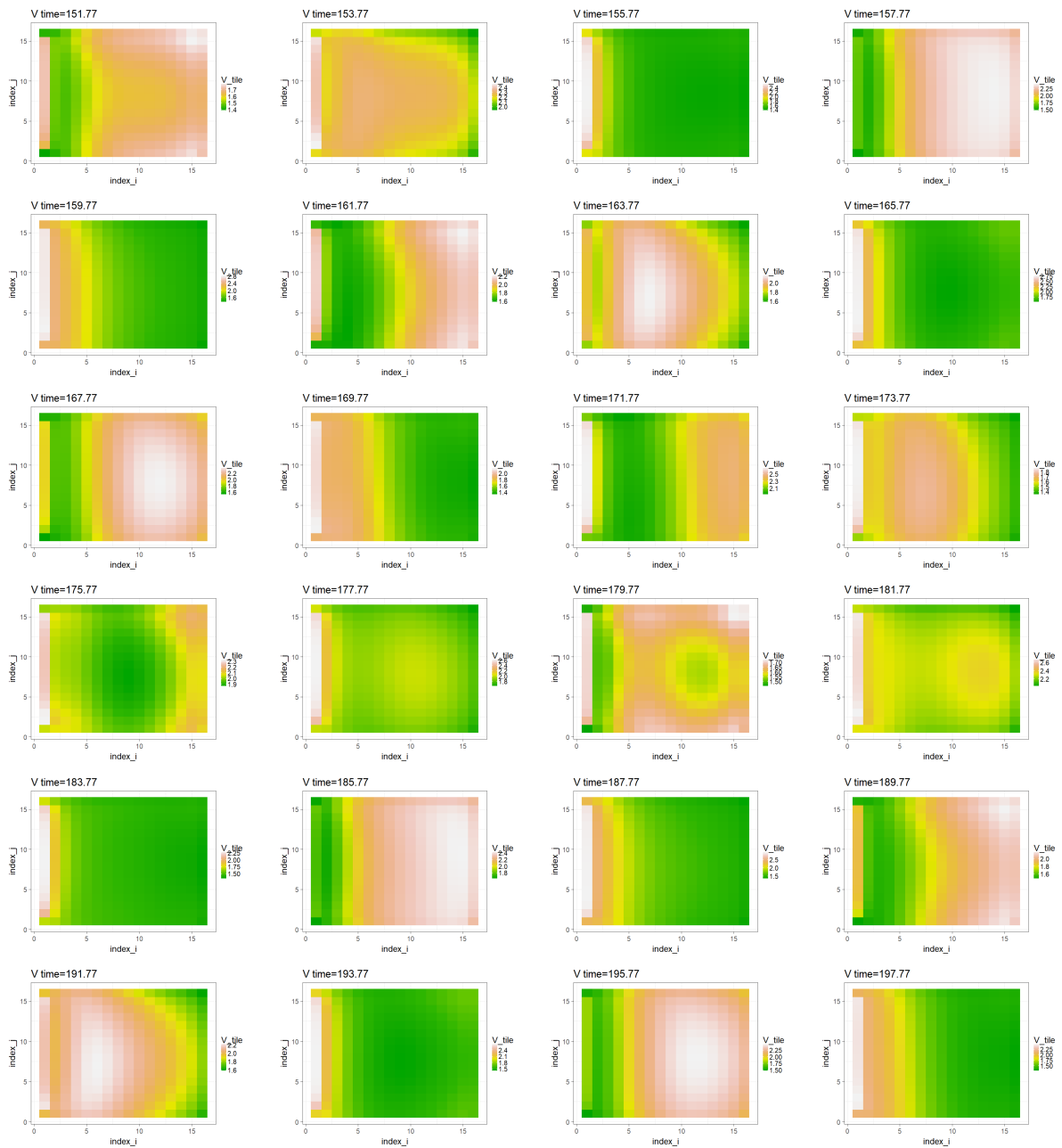
Figure 4.10: Numerical simulation of the system (2.2) at $N = 16$, $n = 0.9$, $\tau = 0.23$. The values of population V.

predict the "bifurcation path to chaos" that we have observed in the numerical simulations. The theory for the bifurcation path to chaos is, of course, well understood for difference equation systems. The authors would greatly appreciate receiving any suggestions that could lead to an analytical understanding of the observed behavior for the lattice differential equation systems.

Our results could be taken into consideration in biosensor design, for fluorescence base biosensor. In this case we can interpret the response time τ as the time after fluorescence emission occurs. The phenomenon of fluorescence occurs when fluorescence labeled antibody (analits) are bind to receptor layer, on which immobilized antigens are found (competitive combination). The faster response (in the form of fluorescent emission) the better stability of the matrix. Therefore, for the values of τ satisfying to conditions of the Theorem 3.1 the stability is observed and this feature may be reached with a higher probability (the biosensor response is cleaner and more readable). As τ increases, the stability is lost until finally chaos occurs.

We have gotten interesting experimental results when taking into account the number of pixels described by the value N. This interpretation can also be related to the increasing number of pixels. We see that amount of pixels in immunosensor narrows the range of τ enabling local asymptotic stability. The higher the number of pixels (e.g., $N = 16$) then the potential binding sites of the antibody with the antigen are more, which also makes the biosensor response "less stable".

We left open problems for the next studies: conditions for global asymptotic stability and the taking into consideration of some biological phenomena of population growth (e.g., Allee effect [31], age-structured growth [3] etc.)

Acknowledgement

References

[1] M. Adivar, Y. N. Raffoul, Inequalities and exponential decay in time varying delay differential equations, *Math. Comput. Modelling* **54**(2011), 794–802. https://doi.org/10.1016/j.mcm.2011.03.027; MR2801932

[2] C. Adley, Past, present and future of sensors in food production, *Foods* **3**(2014), 491–510, https://doi.org/10.3390/foods3030491.

[3] V. Akimenko, R. Anguelov, Steady states and outbreaks of two-phase nonlinear age-structured model of population dynamics with discrete time delay, *J. Biol. Dyn.* **11**(2017), 75–101. https://doi.org/10.1080/17513758.2016.1236988; MR3733427

[4] N. Bairagi, D. Jana, On the stability and Hopf bifurcation of a delay-induced predator–prey system with habitat complexity, *Appl. Math. Model.* **35**(2011), 3255–3267. https://doi.org/10.1016/j.apm.2011.01.025; MR2785276

[5] O. Berg, Orientation constraints in diffusion-limited macromolecular association. The role of surface diffusion as a rate-enhancing mechanism, *Biophys. J.* **47**(1985), 1–14. https://doi.org/10.1016/S0006-3495(85)83870-4

[6] A. BERNOUSSI, A. KADDAR, S. ASSERDA, Stability analysis of an SIRI epidemic model with distributed latent period, *Journal of Advances in Applied Mathematics*, **1**(2016), 211–221. https://doi.org/0.22606/jaam.2016.14002

[7] V. BLOOMFIELD, S. PRAGER, Diffusion-controlled reactions on spherical surfaces. Application to bacteriophage tail fiber attachment, *Biophys. J.* **27**(1979), 447–453. https://doi.org/0.1016/S0006-3495(79)85228-5

[8] S. BOONRANGSIMAN, K. BUNWONG, E. J. MOORE, A bifurcation path to chaos in a time-delay fisheries predator–prey model with prey consumption by immature and mature predators, *Math. Comput. Simulation* **124**(2016), 16–29. https://doi.org/10.1016/j.matcom.2015.12.009; MR3465020

[9] M. BURNWORTH, S. ROWAN, C. WEDER, Fluorescent sensors for the detection of chemical warfare agents, *Chem. Eur. J.* **13**(2007), 7828–7836, https://doi.org/10.1002/chem.200700720

[10] S. R. CHOUDHURY, On bifurcations and chaos in predator–prey models with delay, *Chaos Solitons Fractals* **2**(1992), 393–409. https://doi.org/10.1016/0960-0779(92)90015-F; MR1295920

[11] S.-N. CHOW, J. MALLET-PARET, E. S. VAN VLECK, Dynamics of lattice differential equations, in: *Proceedings of the Workshop on Discretely-Coupled Dynamical Systems, Part I (Santiago de Compostela, 1995), Internat. J. Bifur. Chaos Appl. Sci. Engrg.* **6**(1996), No. 9, 1605–1621. https://doi.org/10.1142/S0218127496000977; MR1434332

[12] H. J. CRUZ, C. C. ROSA, A. G. OLIVA, Immunosensors for diagnostic applications, *Parasitol. Res.* **88**(2002), S4–S7. https://doi.org/10.1007/s00436-001-0559-2

[13] O. DIEKMANN, J. A. P. HEESTERBEEK, J. A. METZ, On the definition and the computation of the basic reproduction ratio R_0 in models for infectious diseases in heterogeneous populations, *J. Math. Biol.* **28**(1990), 365–382. https://doi.org/10.1007/BF00178324; MR1057044

[14] R. D. DRIVER, Existence and stability of solutions of a delay-differential system, *Arch. Rational Mech. Anal.* **10**(1962), No. 1, 401–426. https://doi.org/10.1007/BF00281203; MR0141863

[15] U. FORYŚ, Marchuk's model of immune system dynamics with application to tumour growth, *J. Theor. Med.* **4** (2002), 85–93. https://doi.org/10.1080/10273660290052151

[16] E. FRIDMAN, New Lyapunov–Krasovskii functionals for stability of linear retarded and neutral type systems, *Systems Control Lett.* **43**(2001), 309–319. https://doi.org/10.1016/S0167-6911(01)00114-1; MR2008812

[17] T. D. GIBSON, Biosensors: The stability problem, *Analusis* **27**(1999), 630–638. https://doi.org/10.1051/analusis:1999270630

[18] S. A. GOURLEY, Y. KUANG, J. D. NAGY, Dynamics of a delay differential equation model of hepatitis B virus infection, *J. Biol. Dyn.* **2**(2008), 140–153. https://doi.org/10.1080/17513750701769873; MR2428891

[19] X. HE, Stability and delays in a predator–prey system, *J. Math. Anal. Appl.* **198**(1996), 355–370. https://doi.org/10.1006/jmaa.1996.0087; MR1376269

[20] A. HOFFMAN, H. HUPKES, E. VAN VLECK, *Entire solutions for bistable lattice differential equations with obstacles*, Memoirs of the American Mathematical Society, Vol. 250, 2017. https://doi.org/10.1090/memo/1188; MR3709723

[21] C. HUANG, J. CAO, F. WEN, X. YANG, Stability analysis of SIR model with distributed delay on complex networks, *PloS ONE*, **11**(8)(2016), e0158813. https://doi.org/10.1371/journal.pone.0158813

[22] J. H. JONES, *Notes on $\mathcal{R}_0$*, Department of Anthropological Sciences, Stanford University, California, USA.

[23] A. KŁOS-WITKOWSKA, Enzyme-based fluorescent biosensors and their environmental, clinical and industrial applications, *Pol. J. Environ. Stud.* **24**(2015), 19–25. https://doi.org/10.15244/pjoes/28352.

[24] A. KŁOS-WITKOWSKA, The phenomenon of fluorescence in immunosensors, *Acta. Biochim. Pol.* **63**(2016), 215–221. https://doi.org/10.18388/abp.2015_1231

[25] A. KOROBEINIKOV, A Lyapunov function for Leslie–Gower predator–prey models, *Appl. Math. Lett.* **14**(2001), 697–699. https://doi.org/10.1016/s0893-9659(01)80029-x; MR1836072

[26] A. KOROBEINIKOV, Global asymptotic properties of virus dynamics models with dose-dependent parasite reproduction and virulence and non-linear incidence rate, *Math. Med. Biol.* **26**(2009), 225–239. https://doi.org/10.1093/imammb/dqp006

[27] A. KOROBEINIKOV, Stability of ecosystem: global properties of a general predator–prey model, *Math. Med. Biol.* **26**(2009), 309–321. https://doi.org/10.1093/imammb/dqp009

[28] A. KOROBEINIKOV, W. LEE, Global asymptotic properties for a Leslie–Gower food chain model, *Math. Biosci. Eng.* **6**(2009), 585–590, https://doi.org/10.3934/mbe.2009.6.585; MR2549507

[29] S. KRISE, S. R. CHOUDHURY, Bifurcations and chaos in a predator–prey model with delay and a laser-diode system with self-sustained pulsations, *Chaos Solitons Fractals* **16**(2003), 59–77. https://doi.org/10.1016/S0960-0779(02)00199-6; MR1941157

[30] Y. KUANG, *Delay differential equations with applications in population dynamics*, Academic Press, New York, 1993. MR1218880

[31] E. LIZ, A. RUIZ-HERRERA, Delayed population models with Allee effects and exploitation, *Math. Biosci. Eng.* **12**(2015), 83–97. https://doi.org/10.3934/mbe.2015.12.83; MR3327914

[32] C. LV, Z. YUAN, Stability analysis of delay differential equation models of HIV-1 therapy for fighting a virus with another virus, *J. Math. Anal. Appl.* **352**(2009), 672–683. https://doi.org/10.1016/j.jmaa.2008.11.026; MR2501911

[33] G. MARCHUK, R. PETROV, A. ROMANYUKHA, G. BOCHAROV, Mathematical model of antiviral immune response. I. Data analysis, generalized picture construction and parameters evaluation for hepatitis B, *J. Theoret. Biol.* **151**(1991), 1–40. https://doi.org/10.1016/S0022-5193(05)80142-0

[34] V. MARZENIUK, Taking into account delay in the problem of immune protection of organism, *Nonlinear Anal. Real World Appl.* **2**(2001), 483–496. https://doi.org/10.1016/S1468-1218(01)00005-0; MR1858901

[35] C. C. MCCLUSKEY, Complete global stability for an SIR epidemic model with delay—distributed or discrete, *Nonlinear Anal. Real World Appl.* **11**(2010), 55–59. https://doi.org/10.1016/j.nonrwa.2008.10.014; MR2570523

[36] C. C. MCCLUSKEY, Global stability for an SIR epidemic model with delay and nonlinear incidence, *Nonlinear Anal. Real World Appl.* **11**(2010), 3106–3109. https://doi.org/10.1016/j.nonrwa.2009.11.005; MR2661972

[37] P. MEHROTRA, Biosensors and their applications – a review, *J. Oral Biol. Craniofac. Res.* **6**(2016), 153–159. https://doi.org/10.1016/j.jobcr.2015.12.002

[38] H. MIAO, Z. TENG, Z. LI, Global stability of delayed viral infection models with nonlinear antibody and CTl immune responses and general incidence rate, *Comput. Math. Methods Med.* **2016**, Art. ID 3903726, 21 pp. https://doi.org/10.1155/2016/390372; MR3589511

[39] C. MOINA, G. YBARRA, Fundamentals and applications of immunosensors, in: N. Chiu (Ed.), *Advances in immunoassay technology*, pp. 65–80. https://doi.org/10.5772/36947

[40] L. MOSINSKA, K. FABISIAK, K. PAPROCKI, M. KOWALSKA, P. POPIELARSKI, M. SZYBOWICZ, A. STASIAK, Diamond as a transducer material for the production of biosensors, *Przem. Chem.* **92**(2013), 919–923.

[41] A. NAKONECHNY, V. MARZENIUK, Uncertainties in medical processes control, in: *Coping with uncertainty*, Lecture Notes in Economics and Mathematical Systems, Vol. 581, Springer, Berlin, 2006, pp. 185–192. https://doi.org/10.1007/3-540-35262-7_11; MR2278942

[42] H. NIU, Spreading speeds in a lattice differential equation with distributed delay, *Turkish J. Math.* **39**(2015), 235–250. https://doi.org/10.3906/mat-1404-69; MR3311687

[43] S.-H. PAEK, W. SCHRAMM, Modeling of immunosensors under nonequilibrium conditions: I. Mathematic modeling of performance characteristics, *Anal. Biochem.* **196**(1991), 319–325. https://doi.org/10.1016/0003-2697(91)90473-7

[44] S. PAN, Propagation of delayed lattice differential equations without local quasimonotonicity, *Ann. Polon. Math.* **114**(2015), 219–233. https://doi.org/10.4064/ap114-3-3; MR3371770

[45] A. PRINDLE, P. SAMAYOA, I. RAZINKOV, T. DANINO, L. S. TSIMRING, J. HASTY, A sensing array of radically coupled genetic 'biopixels', *Nature*, **481**(2011), 39–44. https://doi.org/10.1038/nature10722.

[46] J.-P. Richard, Time-delay systems: an overview of some recent advances and open problems, *Automatica J. IFAC* **39**(2003), 1667–1694. `https://doi.org/10.1016/S0005-1098(03)00167-5`; MR2141765

[47] A. Shatyrko, J. Diblík, D. Khusainov, M. Růžičková, Stabilization of Lur'e-type non-linear control systems by Lyapunov–Krasovskii functionals, *Adv. Difference Equ.* **2012**, 2012:229, 9 pp. `https://doi.org/10.1186/1687-1847-2012-229`; MR3018246

[48] J. Sun, G. Liu, J. Chen, D. Rees, Improved delay-range-dependent stability criteria for linear systems with time-varying delays, *Automatica J. IFAC* **46**(2010), 466–470. `https://doi.org/10.1016/j.automatica.2009.11.002`; MR2877095

[49] C. Vargas-De-León, Lyapunov functionals for global stability of Lotka–Volterra cooperative systems with discrete delays, *Abstraction & Application*, **12**(2015), 42–50,

[50] F. Wu, Asymptotic speed of spreading in a delay lattice differential equation without quasimonotonicity, *Electron. J. Differential Equations* **2014**, No. 213, 1–10. MR3273096

[51] R. Xu, M. Chaplain, Persistence and global stability in a delayed predator–prey system with Michaelis–Menten type functional response, *Appl. Math. Comput.* **130**(2002), 441–455. `https://doi.org/10.1016/s0096-3003(01)00111-4`; MR1912224

[52] R. Xu, L. Chen, M. A. J. Chaplain, Persistence and global stability in a delayed predator–prey system with Holling-type functional response, *ANZIAM J.* **46**(2004), 121–141. `https://doi.org/10.1017/s1446181100013729`; MR2075518

[53] R. Xu, Q. Gan, Z. Ma, Stability and bifurcation analysis on a ratio-dependent predator–prey model with time delay, *J. Comput. Appl. Math.* **230**(2009), 187–203. `https://doi.org/10.1016/j.cam.2008.11.009`; MR2532302

[54] J. Yang, X. Wang, F. Zhang, A differential equation model of HIV infection of CD4$^+$ T-cells with delay, *Discrete Dyn. Nat. Soc.* **2008**, Art. ID 903678, 16 pp. MR2476699

[55] G.-B. Zhang, Global stability of traveling wave fronts for non-local delayed lattice differential equations, *Nonlinear Anal. Real World Appl.* **13**(2012), 1790–1801. `https://doi.org/10.1016/j.nonrwa.2011.12.010`; MR2891010